

AR-010-615

OF THE STRESS FIELD

Elastoplastic Analysis of Notch-Tip
Fields in Strain Hardening Materials

Wanlin Guo, C.H. Wang and
L.R.F. Rose

DSTO-RR-0137

19981112 030

☐ APPROVED FOR PUBLIC RELEASE

© Commonwealth of Australia

Elastoplastic Analysis of Notch-Tip Fields in Strain Hardening Materials

Wanlin Guo, C. H. Wang and L. R. F. Rose

**Airframes and Engines Division
Aeronautical and Maritime Research Laboratory**

DSTO-RR-0137

ABSTRACT

The elastic-plastic fields near a notch tip in strain hardening materials are investigated and modelled for a wide range of notch configuration, geometry, and load levels. Two engineering methods that are commonly employed for determining the elastic-plastic response at a notch tip are first assessed, and the results indicate that Neuber's rule and its various extensions tend to overestimate the plastic strain at the notch-tip, and under-estimate the plastic strain away from the notch-tip. By contrast, the ESED method tends to underestimate the plastic strain at the notch-tip and its accuracy deteriorates as the load level increases. It is found that both methods are unable to provide satisfactory predictions of the stress-strain distribution ahead of a notch tip. To this end, an engineering approach is developed to characterise the stress-strain distribution in the notch-tip plastic zone, taking into account of the in-plane and through-thickness constraints near the notch root. Predictions are compared with finite element results, showing a good correlation for all the cases investigated.

RELEASE LIMITATION

Approved for public release

DEPARTMENT OF DEFENCE

DEFENCE SCIENCE AND TECHNOLOGY ORGANISATION

Published by

*DSTO Aeronautical and Maritime Research Laboratory
PO Box 4331
Melbourne Victoria 3001 Australia*

Telephone: (03) 9626 7000

Fax: (03) 9626 7999

© Commonwealth of Australia 1998

AR-010-615

August 1998

APPROVED FOR PUBLIC RELEASE

Elastoplastic Analysis of Notch-Tip Fields in Strain Hardening Materials

Executive Summary

For most load-carrying structures, stress concentration sites are inevitably the most important locations critical to the safety and structural integrity of structures. In particular, the primary structures of modern military aircraft are designed to carry high loads or stresses, plastic deformation near stress concentration sites, such as notches and cut-outs, is of great importance, as it is the plastic deformation that is the driving force for fatigue failure. Therefore, the ability to evaluate the elastic-plastic stress-strain distribution at a notch root is the pre-requisite to durability and damage tolerance analysis, and is consequently of primary importance to the safe management of platforms and development of repair or life extension strategies.

Although it is well known that the stress/strain at the notch tip can be approximately determined using Neuber's rule and the Equivalent Strain Energy Density (ESED) method, there does not exist a method for determining the stress and strain distributions ahead of the notch tip. In the present work, the elastic-plastic notch-tip fields in strain hardening materials are investigated and modelled for a wide range of notch configuration, geometry, and loads. The results suggest that both Neuber's rule and the ESED method fail to give satisfactory predictions of the stress-strain distributions ahead of a notch tip. An engineering approach is proposed to model the stress-strain distribution in the notch plastic zone, accounting for the in-plane and out-of-plane plastic constraints around a notch tip. Comparisons with finite element results demonstrate that the present method correlates well the finite element results.

The solutions presented in this report provide a computationally efficient method for determining the stress/strain distributions ahead of a notch root, which is critical to the damage tolerance analysis of aircraft structures. This is particularly important to the development of in-country damage tolerance analysis support for the RAAF's F-111 fleet.

Authors

Wanlin Guo

Wanlin Guo graduated in 1985 with Bachelor of Engineering (Aeronautical), in 1988 with a Master's degree and in 1991 with a Doctor of Engineering (Mechanical). In recent years he has been active in the field of Strength and Integrity of Structures, three-dimensional fracture and failure theory of structures under complex environment and residual stress analysis. He is a professor and deputy director of the State Key Laboratory of Mechanical Structural Strength and Vibration, Xian Jiaotong University, China. Between April 1997 and April 1998 Prof. Guo worked at the DSTO Centre of Expertise in Structural Mechanics in Monash University.

Chun Hui Wang

Airframes and Engines Division

Dr. Chun H. Wang joined DSTO in 1995 as a Senior Research Scientist. After completing his Ph.D in 1990 at the University of Sheffield, UK, he held various academic positions at Deakin University, the University of Sydney and the University of Sheffield, UK, prior to joining DSTO. His research interests include fatigue and fracture mechanics, bonded joints and repairs, advanced composite materials, constitutive modelling, and cracking of Macadamia nuts.

Francis Rose

Airframes and Engines Division

Francis Rose graduated with a B.Sc (Hons.) from the University of Sydney in 1971 and a Ph.D from Sheffield University, UK in 1975.

He was appointed as a Research Scientist at the Aeronautical Research Laboratory in 1976 and is currently the Research Leader in Fracture Mechanics in the Airframes and Engines Division. He has made important research contributions in fracture mechanics, non-destructive evaluation and applied mathematics. He is the regional Editor for the International Journal of Fracture and a member of the editorial board of Mechanics of Materials. He is also a Fellow of the Institute for Applied Mathematics and its Applications, UK and a Fellow of the Institute of Engineers, Australia.

Contents

NOMENCLATURE	1
1. INTRODUCTION	3
1.1 Stress Concentration at Notch Tips	3
1.1.1 Neuber's rule	4
1.1.2 Equivalent strain energy density method (ESED)	4
1.2 Stress Distribution ahead of Notch Tip	5
2. FORMULATION OF THE PROBLEM	5
2.1 Definition of the Problem	5
1.2 Constitutive Relationships	6
1.3 Strain Energy Density	8
1.4 Stress Distributions ahead of Notch-tips	10
1.4.1 Linear Elastic Notch-Tip Stress Fields	13
1.1.2 Elastic-plastic Notch-tip Fields	14
1.1.3 Assessment of Neuber's Rule and ESED Rule	17
2. PREDICTION OF STRESS-STRAIN DISTRIBUTION	20
2.1 Prediction Model	20
1.2 Application of modified Neuber's rule	22
1.3 Validation of the Model	23
3. CONCLUSIONS	24
4. REFERENCES	35

NOMENCLATURE

E	= Young's modulus
E_s	= secant modulus
ν	= Poisson's ratio
ν_{ep}	= effective Poisson's ratio
n	= strain hardening exponent
σ_{ys}	= yield stress
$\sigma_{eq}, \epsilon_{eq}$	= equivalent stress and equivalent strain
x, y, z	= coordinate with origin being at notch-tip
i, j, k	= indices, $i, j, k=1, 2, 3$, or x, y, z ; summation is implied
x_p	= size of notch plastic zone
ρ	= notch-tip radius
d	= depth of notch
D	= half width of a notched component.
S	= remote stress
λ	= biaxial stress ratio
σ_n	= net section average stress
K_t	= stress concentration factor
$\sigma_{ij}, \epsilon_{ij}$	= stress and strain tensor
δ_{ij}	= Kronecker's delta
$\epsilon_{ij}^e, \epsilon_{ij}^p$	= elastic and plastic parts of total strain ϵ_{ij}
T_z	= out-of-plane stress constraint factor: $\sigma_{zz}/(\sigma_{xx} + \sigma_{yy})$
T_x	= in-plane stress ratio: σ_{xx}/σ_{yy}
W_{EQ}, W_{eq}	= strain energy density defined by $(\sigma_{ij}, \epsilon_{ij})$ and $(\sigma_{eq}, \epsilon_{eq})$
σ_{maxE}	= notch-tip σ_{yy} ($x=0, y=0$) obtained from linear elastic analysis
$()^E$	= elastic solutions

DSTO-RR-0137

1. INTRODUCTION

Stress concentrations in structures are frequently the sites of potential fatigue crack initiation and eventual failure, especially for those designed to carry stresses close their yield stress. In these structures, plastic deformation tends to occur in stress concentration regions, and therefore it is important to accurately determine the elastic-plastic stresses and strains. In the traditional local strain approach to fatigue life prediction, only the stress or strain at the notch tip is required to determine the fatigue initiation life. In this case, empirical methods such as Neuber's rule [1] and the equivalent strain energy density (ESED) method [2] and various extensions [3-8] are frequently used to estimate the elastic-plastic response at a notch-tip on the basis of elastic solutions. However, the stress/strain distributions ahead of a notch tip are pre-requisite to the application of advanced damage tolerance and durability analyses, where the stress distribution along the potential crack path is required to calculate the driving force for fatigue crack growth. Although finite element methods (FEM) are capable of providing the full field stress/strain distribution within a structure, an efficient yet reliable analytical approach is essential to facilitate rapid damage tolerance analysis and to reduce the cost associated with performing detailed elastic-plastic finite element analysis.

Attempts have been made to extend either Neuber's rule or the ESED method to every point ahead of a notch-tip. For example, Ball [9] used a modified Neuber's rule to determine the elastic-plastic stress field ahead of a notch tip. However, the fundamental question surrounding the validity of Neuber's rule when applied to a point ahead of a notch-tip was not addressed, hence it is not clear what causes the failure of existing notch approaches in characterising the notch field.

In this report, Neuber's rule and ESED assumption and their extensions are first assessed with the aid of the finite element method. It is found that these methods are unable to provide satisfactory estimates of the stress-strain distribution in the notch plastic zone. An engineering method is then proposed in which the modified Neuber's rule was used at one point ahead of the notch-tip, and the fields in the plastic zone were then determined based on equilibrium considerations. Whenever possible comparisons are made between the model predictions and finite element results to demonstrate the capabilities of the new approach.

1.1 Stress Concentration at Notch Tips

The severity of stress concentration at a notch root is often measured by the stress concentration factor, defined as the ratio of the stress at the notch tip to the remotely applied nominal stress. Tabulations of the elastic stress concentration factors for a variety of notch geometry and loading configurations have been documented in handbooks (e.g. [10]). For some notch configurations, approximate formulae have also been suggested to estimate the stress concentration factors (e.g. [11,12]).

Under elastic-plastic conditions, several empirical methods are available to estimate the notch-tip stress/strain based on the elastic solutions [12]. The two most popular ones are Neuber's rule [1] and the ESED method [2]. Both of them have been derived for simple stress states in which only one stress component exists at notch-tips. For notched bodies in plane strain and axial-symmetrical problems, extensions of Neuber's rule have been proposed by Topper *et al.* [3], Gemma [4] and Hoffman and Seeger [5], and of the ESED method by Glinka [6], Moftakhar *et al.* [7] and Singh *et al.* [8]. These methods are only briefly outlined in the following.

1.1.1 Neuber's rule

Consider a typical notched component shown in Figure 1, which is subjected to a nominal stress and strain, denoted respectively as S and e . Neuber's rule states that the maximum stress σ and strain ε at the notch root under elastic-plastic deformation are related through the following equation

$$\frac{(K_t S)^2}{E} = \sigma \varepsilon \quad (1)$$

where K_t denotes the elastic stress concentration factor, and E the Young's modulus of the material. Neuber's rule was originally proposed for notched components under plane stress condition, where the stress at the notch-tip is in effect uniaxial. For plane strain condition or general multiaxial stresses, two kinds of extensions have been suggested [5,7]:

$$\sigma_{eq} \varepsilon_{eq} = \sigma_{eq}^E \varepsilon_{eq}^E \quad (2)$$

$$\sigma_{ij} \varepsilon_{ij} = \sigma_{ij}^E \varepsilon_{ij}^E \quad (3)$$

where the superscript E is used to denote the parameters pertaining to the corresponding elastic solutions.

1.1.2 Equivalent strain energy density method (ESED)

This method was also originally proposed to estimate the notch-tip strains under uniaxial stress conditions [2]

$$W^E = \frac{(K_t S)^2}{2E} = W_{EP} = \int_0^{\varepsilon} \sigma d\varepsilon \quad (4)$$

In the case of multiaxial stresses, similar extensions have been proposed [6-8], noting the use of two definitions of the strain energy density (the difference will be discussed later)

$$W^E = \frac{(K_t S)^2}{2E} = W_{eq} = \int_0^{\varepsilon_{eq}} \sigma_{eq} d\varepsilon_{eq} \quad (5)$$

$$W^E = W_{EP} = \int_0^{\varepsilon_{ij}} \sigma_{ij} d\varepsilon_{ij} \quad (6)$$

Moftakhar *et al.* [7] added another equivalent equation of fractional contribution of the total strain energy density in trying to refine these methods to better model the general multiaxial stresses.

It is well recognised that that in most cases Neuber's rule overestimates the notch-tip stresses and strains, while ESED method tends to underestimate the notch stress/strain [13]. Furthermore, the accuracy of these methods depends strongly on the level of the nominal stress relative to the material's yield stress, the material's constitutive law, the stress concentration factor as well as the nature of the stress state.

1.2 Stress Distribution ahead of Notch Tip

The stress distribution ahead of the notch tip is essential to evaluating the stress intensity factors (SIF) of cracks emanating from notches, which represents the driving force for fatigue crack growth. Some authors have proposed direct extension of Neuber's rule and the ESED method to every point ahead of notch-tip, but with little success, the difficulty being that it is no longer appropriate to consider the stress state to be one-dimensional, unlike the situation at the notch tip. Thus the problem in essence is to estimate the rate of increase of the in-plane stress σ_{xx} in Figure 1 with distance from the notch root. Furthermore, even in the case plane stress where there is only one non-zero stress component, there are more than one stress components ahead of the notch-tip, so additional equations are required to fully solve the problem.

In the following sections, Neuber's rule and the ESED method will be first assessed by aid of finite element method. A new approach is then proposed to determine the stress distributions ahead of notch-tip, and the predictions are compared with finite element solutions.

2. FORMULATION OF THE PROBLEM

2.1 Definition of the Problem

Consider the typical notched body as shown in Figure 1, directly ahead of the notch-tip, there are possibly three non-zero stress components. For convenience, let us define an out-of-plane stress constraint factor T_z and an in-plane stress ratio T_x ,

$$T_z = \frac{\sigma_{zz}}{\sigma_{xx} + \sigma_{yy}} \quad (7)$$

$$T_x = \frac{\sigma_{xx}}{\sigma_{yy}} \quad (8)$$

where $T_z=0$ for plane stress and $T_z=\nu$ for plane strain. Here ν denotes the material's Poisson's ratio.

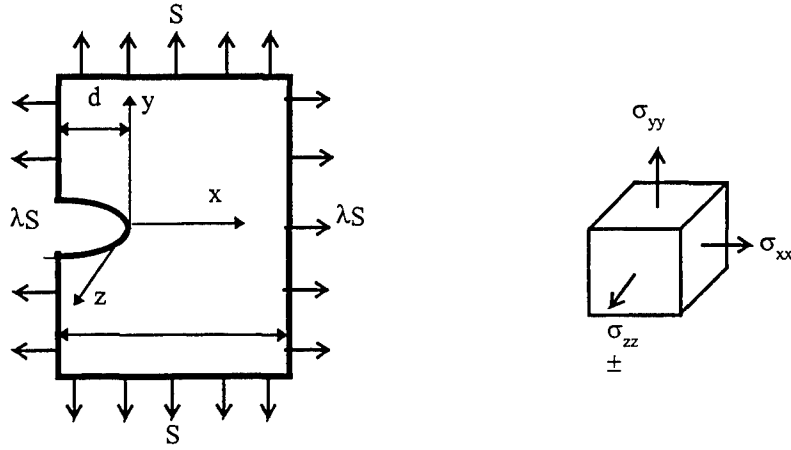


Figure 1: Notations for a notched component subjected to biaxial stresses.

2.2 Constitutive Relationships

According to the deformation theory of plasticity, the total strain ε_{ij} can be decomposed into an elastic part ε_{ij}^e and a volume-preserving plastic part ε_{ij}^p :

$$\varepsilon_{ij} = \varepsilon_{ij}^e + \varepsilon_{ij}^p \quad (9)$$

where the elastic part is related to stress σ_{ij} via Hooke's law:

$$\varepsilon_{ij}^e = \frac{1+\nu}{E} s_{ij} + \frac{1-2\nu}{E} \sigma_m \delta_{ij} \quad (10)$$

where $\sigma_m = \sigma_{ii}/3$, $s_{ij} = \sigma_{ij} - \sigma_m \delta_{ij}$, and

$$\varepsilon_{ij}^p = \frac{3}{2} \left(\frac{1}{E_s} - \frac{1}{E} \right) s_{ij} \quad (11)$$

where E_s represents the yet to be determined secant modulus. Substituting equations (10) and (11) into equation (9), a relationship similar to Hooke's law can be obtained,

$$\varepsilon_{ij} = \frac{1+\nu_{ep}}{E_s} s_{ij} + \frac{1-2\nu_{ep}}{E_s} \sigma_m \delta_{ij} \quad (12)$$

where

$$\nu_{ep} = \frac{1}{2} - \left(\frac{1}{2} - \nu \right) \frac{E_s}{E} \quad (13)$$

Substituting equations (7) and (8) into equation (12) the tension strains can be obtained as

$$\begin{cases} \varepsilon_{xx} = \frac{1}{E_s} [(1 - \nu_{ep} T_z) T_x - \nu_{ep} (1 + T_z)] \sigma_{yy}, \\ \varepsilon_{yy} = \frac{1}{E_s} [(1 - \nu_{ep} T_z) - \nu_{ep} (1 + T_z) T_x] \sigma_{yy}, \\ \varepsilon_{zz} = \frac{1}{E_s} (T_z - \nu_{ep}) (1 + T_x) \sigma_{yy}. \end{cases} \quad (14)$$

The von Mises equivalent stress can be written as

$$\sigma_{eq} = \left(\frac{3}{2} s_{ij} s_{ij} \right)^{1/2} = \left\{ [C_1 (1 + T_x^2) - C_2 T_x] \sigma_{yy}^2 + 3(\sigma_{12}^2 + \sigma_{23}^2 + \sigma_{31}^2) \right\}^{1/2} \quad (15)$$

where parameters $C_1 = 1 - T_z + T_z^2$ and $C_2 = 1 + 2T_z - 2T_z^2$.

The corresponding equivalent strain is

$$\varepsilon_{eq} = \sqrt{\lambda e_{ij} e_{ij}}, \quad e_{ij} = \varepsilon_{ij} - \varepsilon_{kk} \delta_{ij} \quad (16)$$

where the factor λ is introduced to ensure that ε_{eq} is equal to the longitudinal strain in a tensile test. In the fully plastic case, $\lambda=2/3$. Under elastic-plastic situation, the parameter λ is related to the effective Poisson's ratio,

$$\lambda = 3 / [2(1 + 2\nu_{ep} + \nu_{ep}^2)] \quad (17)$$

For simplicity, let us adopt the following power hardening constitutive law; the solutions presented in the following sections can be readily adapted to suit other constitutive models,

$$\varepsilon_{eq} = \frac{\sigma_{eq}}{E} \left(\frac{\sigma_{eq}}{\sigma_{ys}} \right)^{n-1}, \quad (n=1 \text{ for } \sigma_{eq} \leq \sigma_{ys}) \quad (18)$$

which is schematically shown in Figure 2. In this case, the secant modulus and the effective Poisson's ratio can be explicitly expressed in terms of the equivalent stress,

$$\frac{1}{E_s} = \frac{1}{E} \left(\frac{\sigma_{eq}}{\sigma_{ys}} \right)^{n-1}, \quad \nu_{ep} = \frac{1}{2} - \left(\frac{1}{2} - \nu \right) \left(\frac{\sigma_{ys}}{\sigma_{eq}} \right)^{n-1}, \quad (n=1 \text{ for } \sigma_{eq} \leq \sigma_{ys}) \quad (19)$$

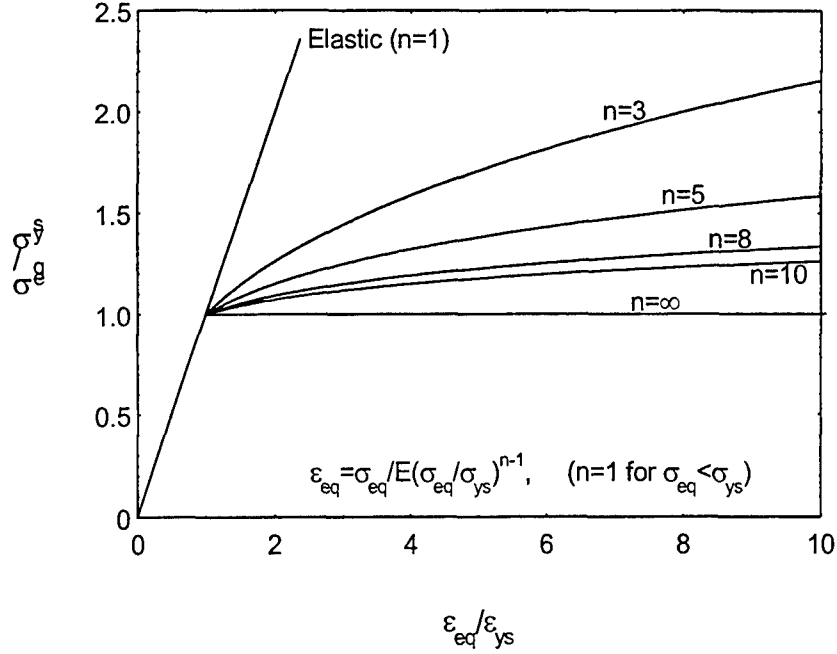


Figure 2: Linear elastic power hardening plastic uniaxial tensile stress-strain relationship

Under plane strain conditions, $\epsilon_{zz} = 0$, the following solution is derived from equation (13)

$$T_z = \nu_{ep} = \frac{1}{2} - \left(\frac{1}{2} - \nu\right) \left(\frac{\sigma_{ys}}{\sigma_{eq}}\right)^{n-1}, \quad (n=1 \text{ for } \sigma_{eq} \leq \sigma_{ys}) \quad (20)$$

In plane stress we have $T_z = 0$. For structures with finite thickness, the average T_z through the thickness may vary between 0 and ν_{ep} , depending on the geometry and loading parameters.

2.3 Strain Energy Density

As discussed in Section 1.1, two different definitions of the strain energy density have been employed in extending Neuber's and the ESED method to multiaxial stresses,

$$W_{EP} = \int_0^{\epsilon_{ij}} \sigma_{ij} d\epsilon_{ij} \quad (21)$$

$$W_{eq} = \int_0^{\epsilon_{eq}} \sigma_{eq} d\epsilon_{eq} \quad (22)$$

While the first definition is the "correct" one for strain energy density, the second definition is easier to compute, for it can be evaluated using the uniaxial stress/strain curve. In the case of linear elastic bodies, substituting equation (10) into the above equations it can be shown that

$$W_{EP} = \frac{1+\nu}{3E} \sigma_{eq}^2 + \frac{3(1-2\nu)}{2E} \sigma_m^2 \quad (23)$$

$$W_{eq} = \frac{\sigma_{eq}^2}{2E} \quad (24)$$

It is clear that the two definitions are indeed different, although the difference is small for low level hydrostatic stress, i.e., $\sigma_m \ll \sigma_{eq}$.

For elastic-plastic bodies,

$$W_{EP} = W(\varepsilon_{ij}^e) + W(\varepsilon_{ij}^p) = \int \sigma_{ij} d\varepsilon_{ij}^e + \int \sigma_{ij} d\varepsilon_{ij}^p \quad (25)$$

where $W(\varepsilon_{ij}^e)$ is already given by equation (21), and $W(\varepsilon_{ij}^p)$ can be obtained by substituting equations (11) and (15) into equation (22), resulting,

$$W(\varepsilon_{ij}^p) = \frac{n}{n+1} \frac{\sigma_{ys}^2}{E} \left[\left(\frac{\sigma_{eq}}{\sigma_{ys}} \right)^{n+1} - 1 \right] - \frac{1}{2} \frac{\sigma_{ys}^2}{E} \left[\left(\frac{\sigma_{eq}}{\sigma_{ys}} \right)^2 - 1 \right] \quad (26)$$

So that

$$W_{EP} = \frac{n}{n+1} \frac{\sigma_{ys}^2}{E} \left[\left(\frac{\sigma_{eq}}{\sigma_{ys}} \right)^{n+1} - 1 \right] - \frac{1}{2} \frac{\sigma_{ys}^2}{E} \left[\left(\frac{\sigma_{eq}}{\sigma_{ys}} \right)^2 - 1 \right] + \frac{1+\nu}{3} \frac{\sigma_{eq}^2}{E} + \frac{3(1-2\nu)}{2E} \sigma_m^2 \quad (27)$$

where the last term is the dilatation part of the strain energy density and the rest is the distortional part.

From equations (18) and (22), it is easy to show that

$$W_{eq} = \frac{\sigma_{ys}^2}{E} \left[\frac{1}{2} + \frac{n}{n+1} \left(\left(\frac{\sigma_{eq}}{\sigma_{ys}} \right)^{n+1} - 1 \right) \right] \quad (28)$$

Therefore the difference between W_{EP} and W_{eq} is

$$W_{EP} - W_{eq} = \frac{1-2\nu}{6E} (9\sigma_m^2 - \sigma_{eq}^2) \quad (29)$$

Directly ahead of notch tip, i.e., on the plane $y=0$, the shear stress is zero ($\sigma_{xy}=0$), so from equations (15), (28) and (29) we get

$$\frac{W_{EP} - W_{eq}}{W_{eq}} = \frac{(1-2\nu)}{3} \left[\frac{(1+Tz)(1+Tx)}{C_1(1+Tx^2) - C_2Tx} - 1 \right] \quad (30)$$

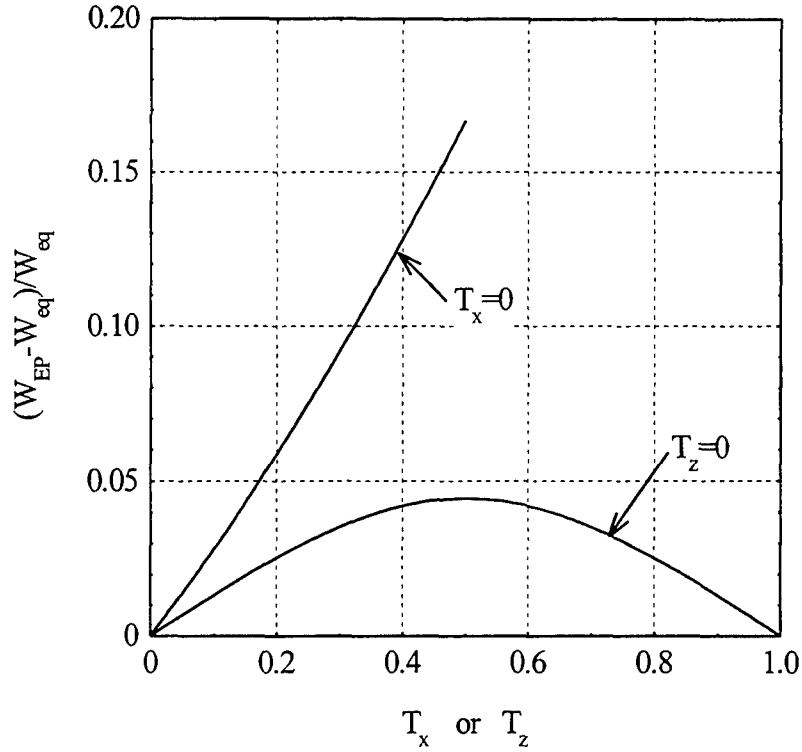


Figure 3: Differences between two strain energy density formulations.

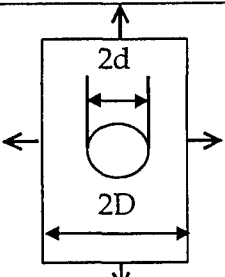
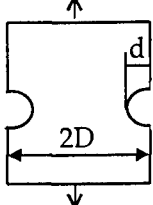
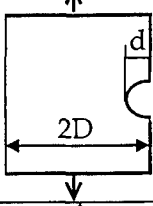
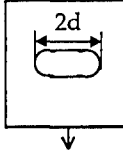
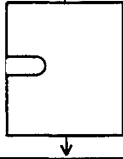
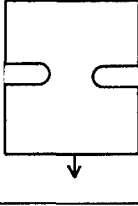
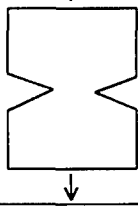
This ratio is shown in Figure 3 in terms of the non-dimensional parameters T_x and T_z . As seen in the figure, under *plane stress* condition, the maximum difference between the two formulations is less than 5%. Under *plane strain* condition, with the increase in the plastic yielding, T_z increases from ν to 0.5, resulting in a difference up to 17%. Therefore, it can be concluded W_{eq} can be used as reasonable approximation for W_{EQ} for the whole range of in-plane or through-thickness constraint.

2.4 Stress Distributions ahead of Notch-tips

To examine the common features of notch-tip fields, seven different types of notch geometry as listed in Table 1 have been analysed by FEM under both plane stress and plane strain conditions. For elastic-plastic calculations, a small strain, J_2 incremental theory of plasticity was used in the FEM analysis. The material was assumed to be homogeneous, isotropic and to obey von Mises yield criterion and Prandtl-Reuss flow rule. The response of the material in uniaxial tension is characterised by a linear-power hardening law of the same form as equation (17). The ratio of the yield stress to the Young's modulus is taken to be 1/2000 and Poisson's ratio is assumed to be 0.3 in all the cases; stress results will be normalised by the material's yield stress σ_{ys} . The models were meshed with 8-node iso-parametric elements. The meshes near the notch tip are sufficiently fine to capture the stress/strain concentration. As shown in Table 1, the stress concentration factors obtained by the FE method under elastic conditions are in

close agreement with those documented in the literature [10]. Here the stress concentration K_m is defined as σ_{\max} / σ_n and $\sigma_n = [D / (D - d)] \sigma_{\text{applied}}$ with D and d denoting respectively the half-width of plate and the half-depth of the notch.

Table 1 Type of notches being considered

	<p><u>Centre circular hole, $D/d=10$, $\rho/d=1$, $K_{tn}=2.7201$ (2.72*).</u></p> <p>Case 1: Plane strain, $n=10$, $\lambda=0$. Case 11: Plane strain, $n=3$, $\lambda=0$. Case 12: Plane stress, $n=8$, $\lambda=0$. Case 13: Biaxial tension ($\lambda=1$), $K_{tn}=1.8362$ Plane strain, $n=10$.</p>
	<p><u>Opposite semi-circular edge notches, $D/d=10$, $\rho/d=1$, $K_{tn}=2.75$ (2.75*)</u></p> <p>Case 2: Plane strain, $n=10$.</p>
	<p><u>Single edge notch, $D/d=10$, $\rho/d=1$, $K_{tn}=2.7553$ (2.75*)</u></p> <p>Case 3: Plain strain, $n=10$</p>
	<p><u>Centre U-notch, $D/d=3$, $\rho/d=0.54$, $K_{tn}=2.8027$ (2.8*)</u></p> <p>Case 4: Plane strain, $n=10$. Case 41: Plane strain, $n=3$. Case 42: plane stress, $n=8$.</p>
	<p><u>Single edge U-notch, $D/d=3$, $\rho/d=0.54$, $K_{tn}=2.3928$ (2.4*)</u></p> <p>Case 5: Plane strain, $n=10$</p>
	<p><u>Double edge U-notch, $D/d=3$, $\rho/d=0.54$, $K_{tn}=2.58$</u></p> <p>Case 6: Plane strain, $n=10$ Case 61: Plane strain, $n=3$ Case 62: Plane stress, $n=8$</p>
	<p><u>Double V-shaped notches, $D/d=1.8$, $\rho/d=0.144$, $K_t=3.246$</u></p> <p>Case 7: Plane strain, $n=10$. Case 71: Plane strain, $n=3$. Case 72: plane stress, $n=8$ & 10.</p>

* Peterson's stress concentration factor after [10].

2.4.1 Linear Elastic Notch-Tip Stress Fields

Efforts have been devoted to construct approximate expressions for stress distribution ahead of a notch-tip in elastic bodies [11-12]. Critical assessment of these expressions can be found in [13]. More recently, Lazzarin and Tovo [14] obtained a set of unified solution for cracks and V-notch with circular root.

The best known expressions for calculating stresses in the vicinity of a notch-tip are those derived for circular and elliptical notches in an infinite plate under remote loading. When the stress concentration factor K_t is introduced, the stress components in the plane $y=0$ (see Figure 1) in an infinite plate having a circular hole can be obtained under biaxial loading condition from the classical solution [15]:

$$\sigma_{xx} = \frac{K_t S}{3-\lambda} \left[\lambda + \frac{3-5\lambda}{2} \left(\frac{x}{\rho} + 1 \right)^{-2} - \frac{3(1-\lambda)}{2} \left(\frac{x}{\rho} + 1 \right)^{-4} \right] \quad (31)$$

$$\sigma_{yy} = \frac{K_t S}{3-\lambda} \left[1 + \frac{1+\lambda}{2} \left(\frac{x}{\rho} + 1 \right)^{-2} + \frac{3(1+\lambda)}{2} \left(\frac{x}{\rho} + 1 \right)^{-4} \right] \quad (32)$$

where the parameter λ is the biaxiality ratio. Equations (31-32) can be modified by the approach proposed by Glinka and Newport [12] to take into account of the bending effect,

$$\sigma_{xx} = \frac{K_t S}{3-\lambda} \left[\lambda + \frac{3-5\lambda}{2} \left(\frac{x}{\rho} + 1 \right)^{-2} - \frac{3(1-\lambda)}{2} \left(\frac{x}{\rho} + 1 \right)^{-4} \right] \left(1 - \frac{x}{\kappa} \right) \quad (33)$$

$$\sigma_{yy} = \frac{K_t S}{3-\lambda} \left[1 + \frac{1+\lambda}{2} \left(\frac{x}{\rho} + 1 \right)^{-2} + \frac{3(1+\lambda)}{2} \left(\frac{x}{\rho} + 1 \right)^{-4} \right] \left(1 - \frac{x}{\kappa} \right) \quad (34)$$

Where κ is the distance from notch tip to the neutral axis of the notched component, i.e., the y stress changes sign under bending. For centre notched and double edge notched specimens listed in Table 1, $\kappa \rightarrow \infty$. For single edge notched strip under tension,

$$\kappa = (D-d) \left(\frac{1}{2} + \frac{1}{6} \frac{D-d}{d} \right) \quad (35)$$

As reported by Glinka and Newport [12], Creager and Paris' solution for blunt cracks can be used to estimate stress distribution near the tip of relatively sharp, deep notches:

$$\sigma_{xx} = \frac{K_t S}{2\sqrt{2}} \left[\left(\frac{x}{\rho} + \frac{1}{2} \right)^{-1/2} - \frac{1}{2} \left(\frac{x}{\rho} + \frac{1}{2} \right)^{-3/2} \right] \quad (36)$$

$$\sigma_{yy} = \frac{K_t S}{2\sqrt{2}} \left[\left(\frac{x}{\rho} + \frac{1}{2} \right)^{-1/2} + \frac{1}{2} \left(\frac{x}{\rho} + \frac{1}{2} \right)^{-3/2} \right] \quad (37)$$

Comparison of Eqs.(31-32) and (36-37) with FE results is given in Figure 4 for the stress σ_{yy} and in-plane stress ratio $T_x = \sigma_{xx}/\sigma_{yy}$. It can be seen that the above approximate expressions provide reasonably good estimates of both the y -stress and the in-plane

stress ratio. For shallow notches with $d/\rho \approx 1$ and $D/d \gg 1$, Equations (31-32) are quite accurate. For deep notches with large d/ρ and/or small D/d , the stress distributions ahead of edge notches are better approximated by equations (36-37). For edge notches, proper combination of equations (31-32) and equations (36-37) can lead to better prediction. Thus, the following empirical formula is proposed here,

$$(\sigma_{xx}, \sigma_{yy}) = (1 - \eta)(\sigma_{xx}, \sigma_{yy})_{eq.(31,32)} + \eta(\sigma_{xx}, \sigma_{yy})_{eq.(36,37)} \quad (38)$$

Where,

$$\eta = \frac{\xi}{\xi + \rho/d}, \quad \xi = \frac{d}{D-d} \quad (39)$$

As shown by the solid line in Figure 4, with equation (38) the effects of d/ρ and D/d on the distributions of σ_{yy} and T_x better estimates can be achieved over the region $0 \leq x/\rho \leq 3$. For centre notch in a finite width plate, equation (31) can be used directly if $D/d \geq 3$.

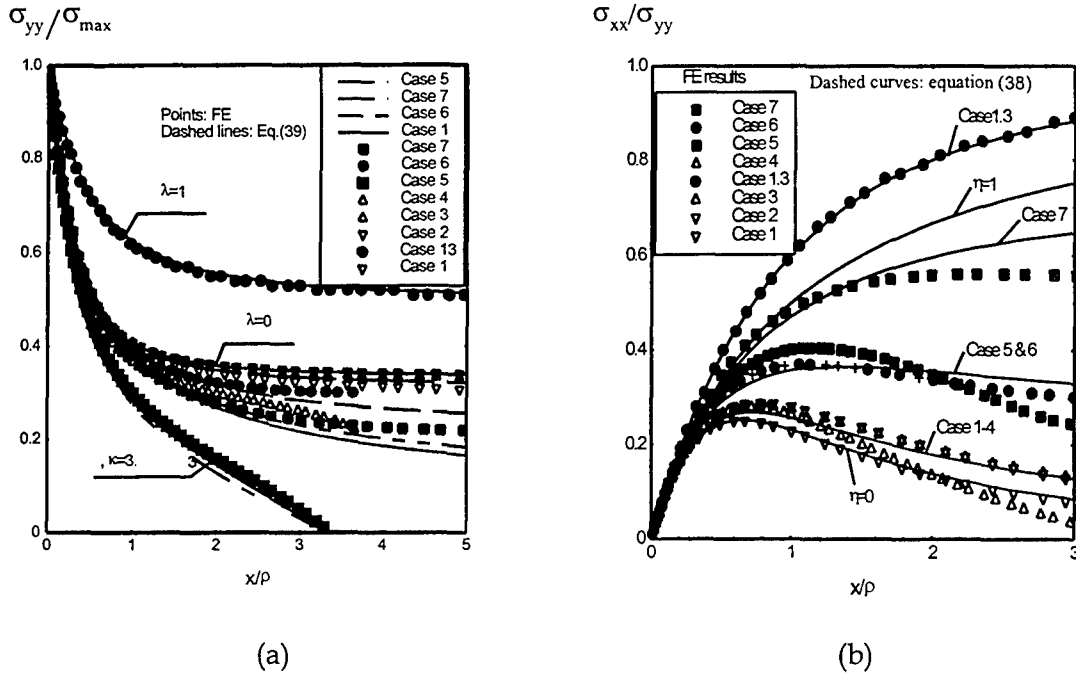


Figure 4: Distributions of elastic stresses ahead of notch-tips; (a) Normalised stress σ_{yy} ahead of notch tip, (b) In-plane stress ratio ahead of notch tip.

2.4.2 Elastic-plastic Notch-tip Fields

Plastic yielding will invariably occur if the remotely applied stress exceeds a certain level, and the resulting stress distributions will deviate from the corresponding elastic case. Figures 5 and 6 show the elastic-plastic notch-tip fields of notch case 1 (under plane strain condition) at various stress levels. It is seen in Figure 5 that with the increase of the nominal stress (σ_n/σ_{ys}), the in-plane stress ratio T_x increases slightly

beyond $x/\rho=0.3$, while the tensile stress σ_{yy} at the notch-tip decreases. The small change in T_x suggests that the two in-plane stress components remain approximately proportional during the plastic deformation. By contrast, the out-of-plane constraint (T_z) at the notch-tip increases considerably from the Poisson's ratio ($\nu=0.3$) to $\frac{1}{2}$ (see Figure 5). Therefore the elastic solution is apparently inadequate for determining the elastic-plastic stress distribution in the notch-tip fields. A new method is called for to account for this stress redistribution resulting from plastic deformation.

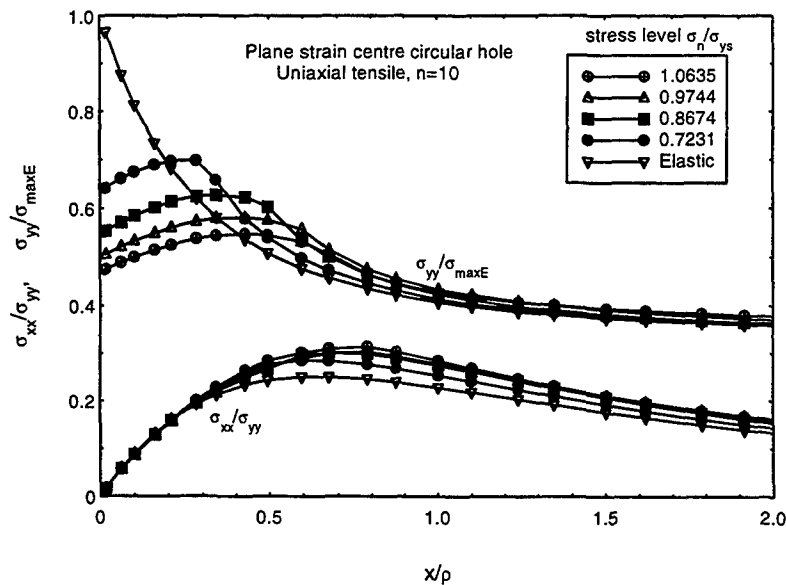


Figure 5: Distribution of elastic-plastic stresses ahead of notch-tip for CASE 1.

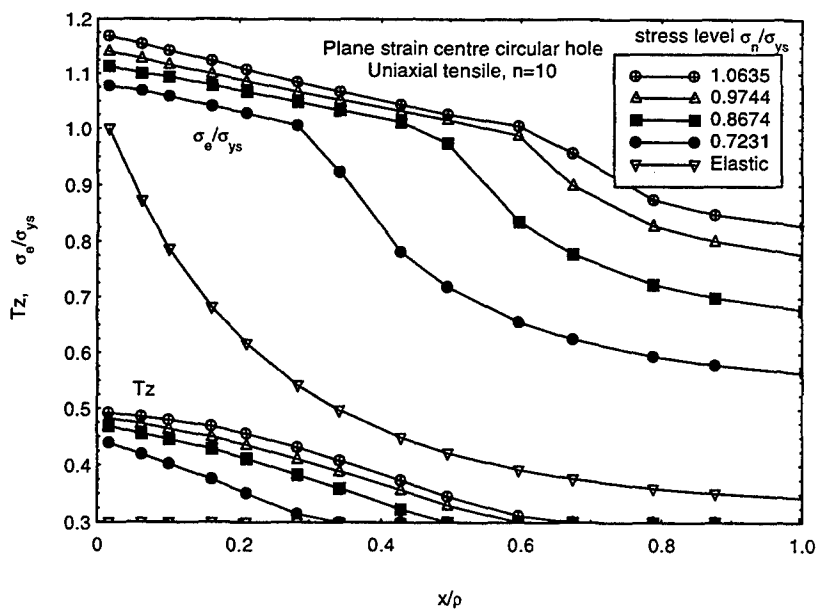


Figure 6: Equivalent stress and constraint factor T_z ahead of the notch-tip in CASE 1

Figure 7 shows the distributions of T_x ahead of notch-tip for all the cases being examined. It is interesting to note that the distribution of T_x within the notch plastic zone is far less sensitive to the notch geometry, load levels and stress states, especially at a small distance from the notch tip. For deeper edge notches (Case 5 to 7.2) and centre notch under biaxial loading (Case 1.3), the distribution of T_x in the plastic zone fall almost onto the slip-line field solution [16], as shown in Figure 7

$$T_x = \frac{\ln(1 + x / \rho)}{1 + \ln(1 + x / \rho)} \quad (40)$$

where x is distance measured from the notch-tip. By contrast, for centre notches and shallow edge notches (Case 1 to 4.2), the data lie close to that of Case 1.2 in net section yield.

For all the cases listed in Table 1, the difference between elastic and elastic-plastic T_x as shown in Figure 7 is less than 22%, so as a simple approximation, the hypothetical elastic solutions of T_x can be used to predict elastic-plastic notch-tip fields. This is in effect assuming that the two in-plane stress components remain proportional during plastic deformation. Improved correlation can be obtained by curve fitting the elastic-plastic solution of T_x . For example, the results of case 12 under net section yielding can be well approximated by the following expression with accuracy better than 1 per cent,

$$T_x = A \frac{x}{\rho} + B \left(\frac{x}{\rho} \right)^2 + C \left(\frac{x}{\rho} \right)^3, \quad (\text{for } x / \rho \leq 2) \quad (41)$$

where $A=8825$, $B=-0.7342$, $C=0.1685$. As shown by Figure 7, equation (41) can be used for very shallow notches.

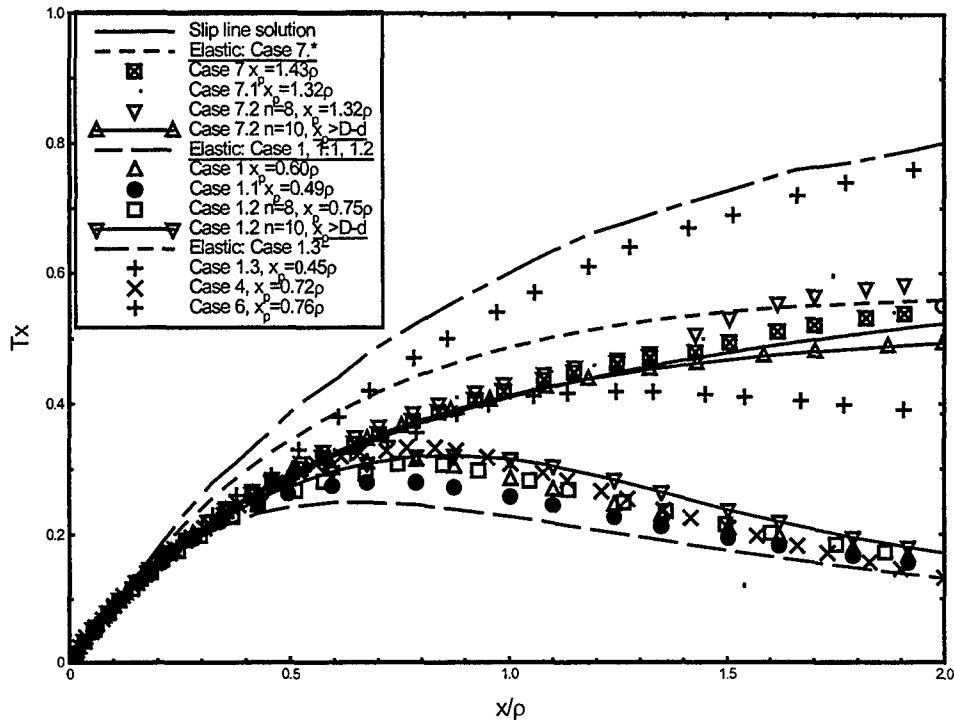
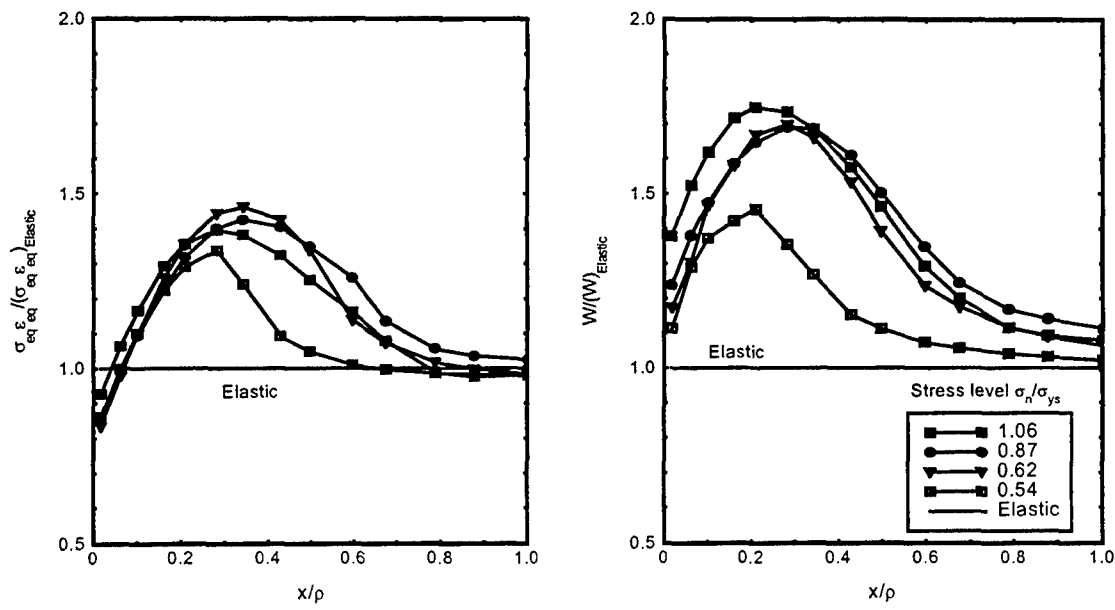


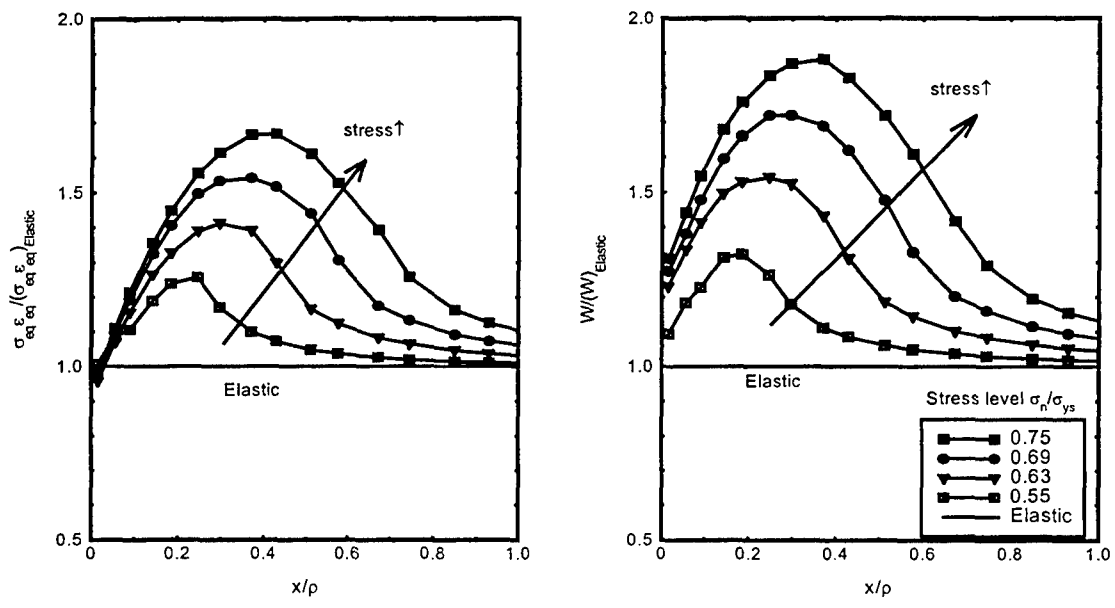
Figure 7: Distributions of the ratio T_x ahead of notch-tip under elastic-plastic condition.

2.4.3 Assessment of Neuber's Rule and ESED Rule

To examine the capabilities of Neuber's rule and the ESED method in evaluating the stresses ahead of notch tip, the predictions based on Neuber's rule and the ESED method for the case of a centre circular hole are shown in Figure 8. The parameters σ_{eq} and W are normalised respectively by their *hypothetical* elastic values. Two observations can be made here. Firstly, the normalised ratios significantly exceed unity, an expected ratio for Neuber's rule or the ESED method to be valid. This clearly demonstrates the failure of both methods to predict the distribution of stresses and strains ahead of the notch-tip. Secondly, the normalised ratios at a given distance ahead of the notch-tip exhibit a dependence on the level of the applied loads. This implies that the plastic deformation at the notch root is causing significant stress redistribution ahead of the notch tip.



(a) plane strain condition



(b) plane stress condition

Figure 8: Neuber's Rule and ESED method for centre circular notch under (a) plane strain and (b) plane stress conditions.

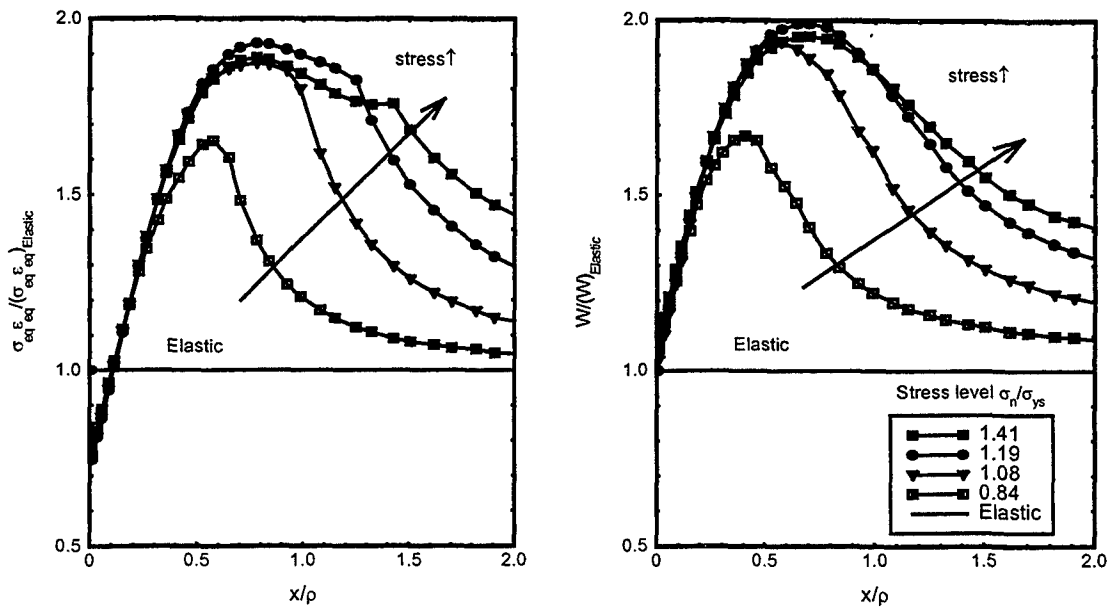


Figure 9: Neuber's rule and ESED method for a V-notch (Case 7).

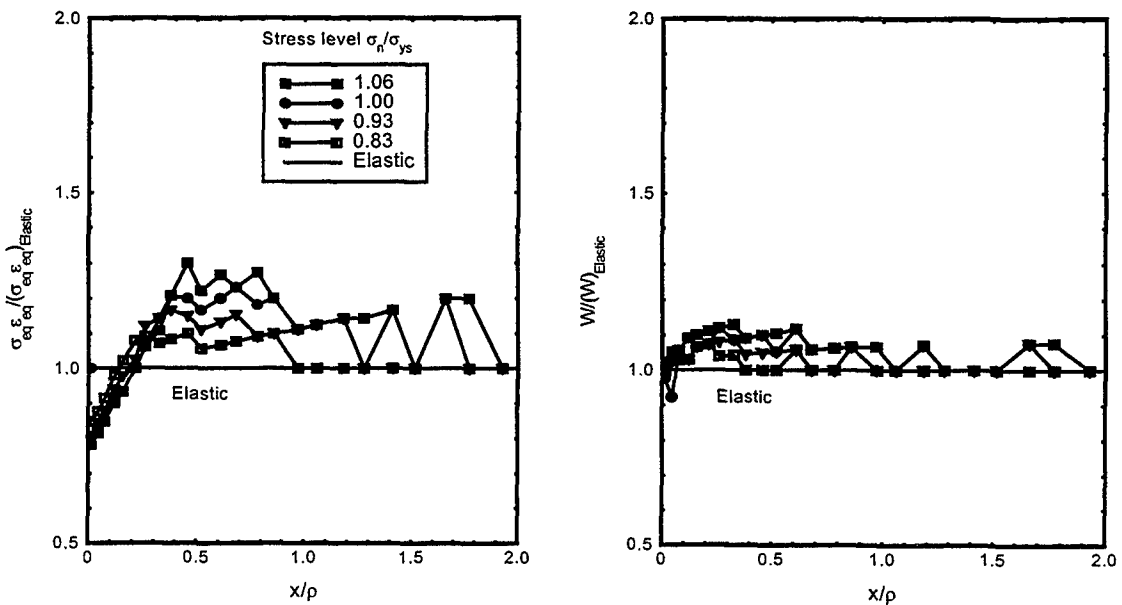


Figure 10: Neuber's rule and ESED method for centre circular notch under biaxial tensile, plane strain (Case 13)

Figures 9 show the results for a V-notch with a semi-circular tip of radius ρ . The parameters σ_{eq} and W are normalised respectively by their hypothetical elastic values. It is seen that the ratios deviate significantly from unity, contrary to what

would be expected from Neuber's rule and the ESED method. At the notch-tip ($x=0$), the normalised parameter $\sigma_{eq}\epsilon_{eq}$ is lower than the hypothetically elastic ones, suggesting that Neuber's rule and its extension will over-estimate the notch-tip strains. By contrast, the normalised strain energy density W exceeds the hypothetical elastic values, consequently the ESED method would under-estimate the notch-tip strains. This suggests that the average of the two predictions may provide an improved prediction of the notch-tip strains.

Under biaxial loading, however, the deviation from unity (see Figure 10) is less pronounced than the two cases shown in Figures 8 and 9. This means that Neuber's rule and the ESED method may yield a better prediction. It is interesting to note in Figures 8 and 9 that the curves of normalised $\sigma_{eq}\epsilon_{eq}$ intersect with the corresponding elastic curve at nearly the same point about $x/\rho = 0.06$. This feature will be exploited later for improving the accuracy of Neuber's rule.

3. PREDICTION OF STRESS-STRAIN DISTRIBUTION

In this section, an engineering method will be developed to predict the stress-strain distribution ahead of a notch tip based on the elastic solutions. All the analysis will be limited to the net section, or along the plane $y=0$.

3.1 Prediction Model

By inspecting the distribution of the equivalent stress within the plastic zone obtained by FE analyses, it is postulated that the equivalent stress in the plastic zone ahead of a notch-tip can be well approximated by a rational function,

$$\frac{\sigma_{eq}(x)}{\sigma_{ys}} = \frac{A}{x + \alpha} \quad (42)$$

where the parameters A and t can be determined by making use Neuber's rule (or the ESED method) and an equilibrium condition as outlined below.

The continuity of the equivalent stress the elastic and plastic boundary, $x=x_p$, leads to

$$A = x_p + \alpha \quad (43)$$

where x_p denotes the plastic zone size, which will be determined later. The parameter α can be inferred by making use Neuber's rule (or the ESED method) at the notch root. For material obeying the power-law strain hardening given by equation (18), the following relationship can be derived,

$$\alpha = \frac{x_p}{B^{1/(1+n)} - 1} \quad (44)$$

where

$$B = \begin{cases} \left(\frac{K_T \sigma_n}{\sigma_{ys}} \right)^2 & \text{(Neuber's rule)} \\ \frac{n+1}{2n} \left[\left(\frac{K_T \sigma_n}{\sigma_{ys}} \right)^2 - 1 \right] + 1 & \text{(ESSED method)} \end{cases} \quad (45)$$

Now with equation (46) the equivalent stress at position x can be expressed as

$$\frac{\sigma_{eq}(x)}{\sigma_{ys}} = \frac{x_p B^{1/(1+n)}}{x B^{1/(1+n)} + (x_p - x)} \quad (46)$$

The plastic zone size x_p is the only remaining unknown. A first order estimate of x_p can be made by equating the hypothetical elastic stress to the yield stress,

$$\sigma_{eq}^E(x_{p0}) = \sigma_{ys} \quad (47)$$

where x_{p0} denotes the first order estimate of the plastic zone size. In doing so the effect of the stress redistribution induced by the plastic deformation has been ignored, and the estimated x_{p0} is expected to be smaller than the actual extent of the plastic deformation. Improvement can be achieved by using a method similar to that proposed by Irwin [17] for sharp cracks. The basic idea is that the occurrence of plasticity makes the notch behave as if it were deeper than its physical size. The effective notch size (d_{eff}) is equal to the $d + x_{p0}$, and the actual plastic size is x_p . In Figure 11, the elastic stress distribution at the tip of the effective notch is the same as that for the original notch except that the origin of the coordinate is shifted to o' as shown in Figure 11(a). Overall equilibrium requires that the load carried by the net section should remain the same, in other words, the areas of the hatched regions in Figures 11(b) and (c) should be equal. This can be mathematically expressed as,

$$\int_0^{x_p} \sigma_{yy}(x) dx = \int_0^{x_p - x_{p0}} \sigma_{yy}^E(x) dx \quad (48)$$

where the y -stress ahead of the notch tip is given by, noting equation (15)

$$\sigma_{yy} = \sigma_{eq}(x) / g(T_z, T_x) \quad (49)$$

with

$$g(T_z, T_x) = \left[(1 - T_z + T_z^2)(1 + T_x^2) - (1 + 2T_z - 2T_z^2)T_x \right]^{1/2} \quad (50)$$

and T_z being given by equation (20). It should be noted that v_{ep} can be evaluated using equation (19).

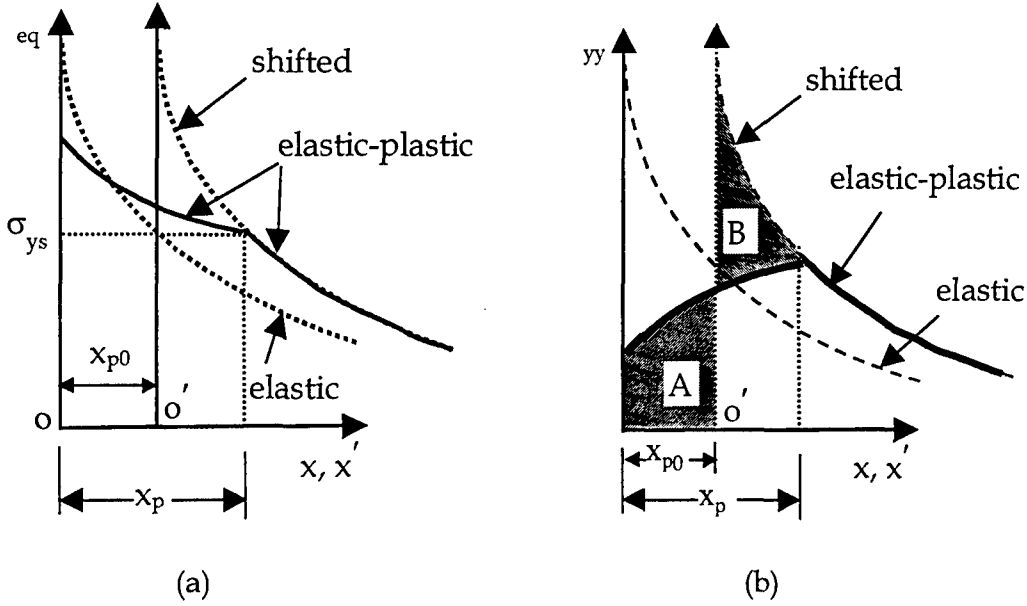


Figure 11: Model of elastic-plastic zone and stress relationships

Due to the complexities of T_x , no closed-form solution of the integral on the left-hand side of equation (50) is possible, however, the only unknown in the equation is x_p , which can be readily obtained numerically by means of Newton-Raphson's method using x_{p0} as an initial guess. Once x_p is determined, the equivalent stress and the y -stress can be determined respectively from equations (48) and (51), for the in-plane stress ratio T_x is well approximated by either the corresponding elastic solution or the slip-line field solution given by equation (40). The y -strain is given by

$$\varepsilon_{yy} = \frac{1+T_z}{E} \left(\frac{\sigma_{eq}}{\sigma_{ys}} \right)^{n-1} [(1-T_z) - T_z T_x] \sigma_{yy} \quad (51)$$

Other stress and strain components can be obtained from equation (14).

3.2 Application of modified Neuber's rule

Since the previous analyses have found that the original Neuber's rule tends to overestimate the stresses and strains at notch-tip, one simple improvement would be to re-cast Neuber's rule at a distance x_0 ahead of the notch-tip, i.e.

$$\sigma_{eq} \varepsilon_{eq} = \frac{[\sigma_{eq}^E(x_0)]^2}{E} \quad (52)$$

which leads to

$$B = \left(\frac{\sigma_{eq}^E(x_0)}{\sigma_{ys}} \right)^2 \quad (53)$$

The previous analyses suggest that $x_0 \approx 0.06\rho$ for the cases being studied. The analysis then follows exactly that outlined in Section 4.1.

3.3 Validation of the Model

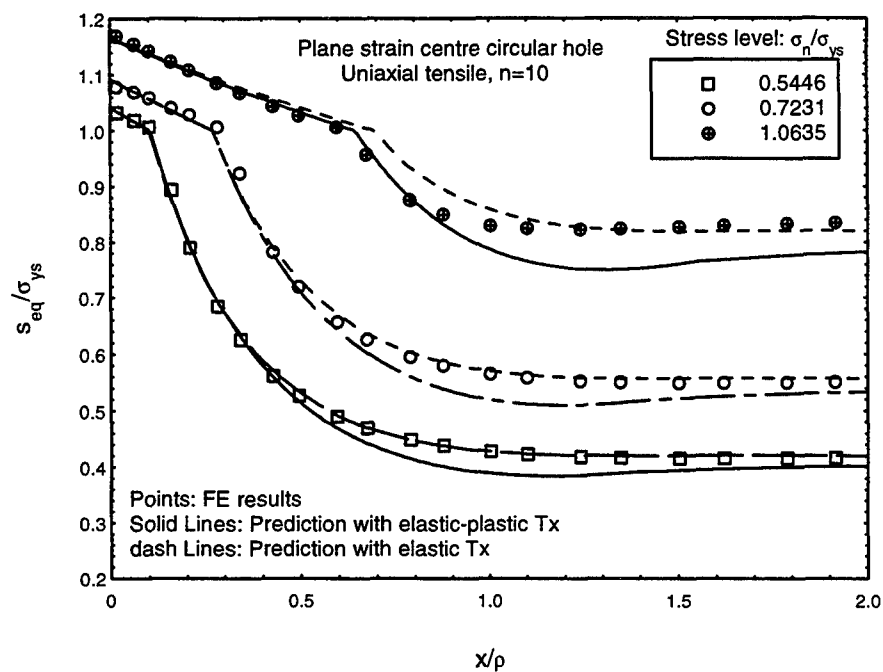
To verify the proposed method, stress and strain distributions ahead of notch-tips have been predicted for the cases listed in Table 1 and results are compared with the FE calculations as shown in Figures 12 to 20. In these figures, symbols represent FE results, and lines denote predictions. In particular, dashed lines represent the predictions made using elastic T_x while solid lines represents predictions made using the empirical expression of T_x given by equation (41). Except for the biaxial tension case, the modified Neuber's rule is employed at $x/\rho=0.06$. Figures 12 show the results for a centre circular hole in a relatively wide plane strain strip with the material having a strain hardening exponent $n=10$. When the stress level σ_n / σ_{ys} is lower than 0.8, use of both the elastic T_x and the elastic-plastic T_x yields nearly the same predictions. For higher applied stress, better predictions are obtained if the elastic-plastic T_x is employed.

As shown in Figures 12(a), 15(a), and 19(a), the postulated functional relation of the equivalent stress does provide a good correlation with the FE results within the whole plastic zone. As shown in Figure 16, the agreement between the predictions and the FE results seems to improve for materials exhibiting strong strain hardening (smaller strain hardening exponent). So comparisons for other cases with $n=3$ will not be discussed in the following.

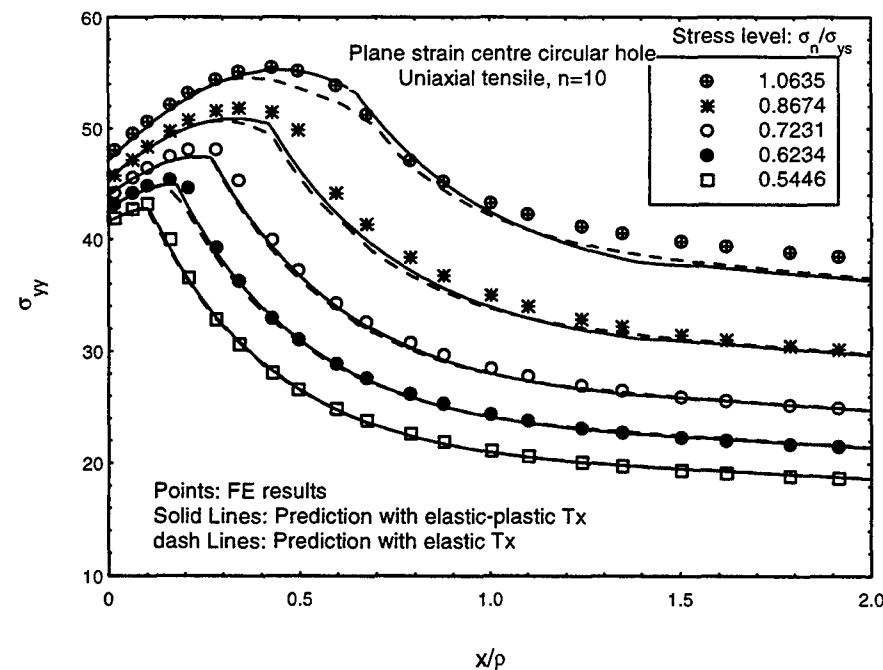
It should be pointed that the present method is applicable only when the plastic deformation around the notch root is constrained, viz, the plastic zone size is smaller or comparable to the notch root radius. This is because under large scale yielding, neither Neuber's rule nor the ESED method is able to predict the responses at notch-tip [18]. Two examples under plane stress conditions are shown in Figures 21 and 22, indicating a significant under-estimation of the strain distributions. In practical applications, however, such cases are relatively rare as most structures would not be designed to operate under such high stresses.

4. CONCLUSIONS

1. Both Neuber's rule and the ESED method have been found to significantly underestimate the distributions of stress and strain ahead of a notch tip, although these two methods can yield reasonable predictions of the notch-tip response.
2. Within the notch plastic zone, the two in-plane stress components are found to remain approximately proportional, allowing the direct application of the elastic solutions for the in-plane stress ratio.
3. A new method has been developed to determine the stresses and strains ahead of a notch tip; comparisons with finite element results demonstrate that the predictions of the method are in close agreement with the FE results.
4. The new method is also able to predict the size of the notch plastic zone.



(a) prediction of equivalent stress σ_{eq}



(b) prediction of stress σ_{yy}

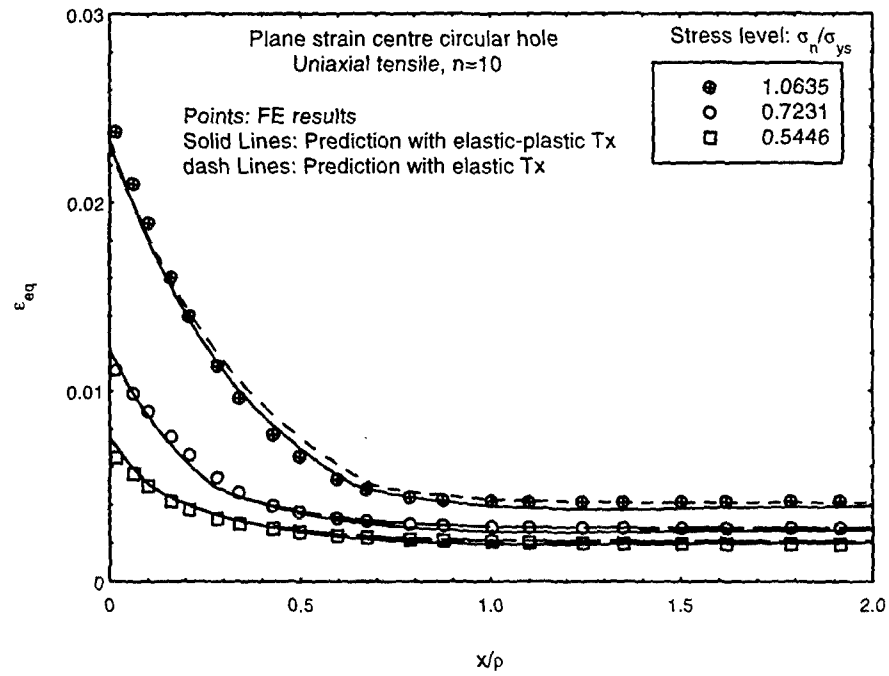
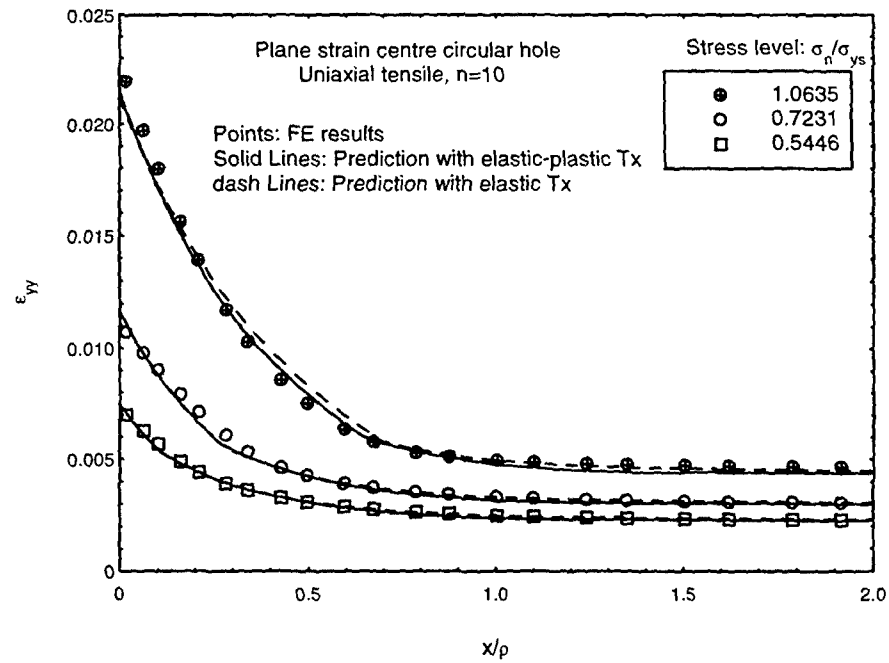
(c) prediction of equivalent strain ϵ_{eq} (d) prediction of strain ϵ_{yy}

Figure 12: Prediction of stress-strain fields ahead of the notch-tip in CASE 1

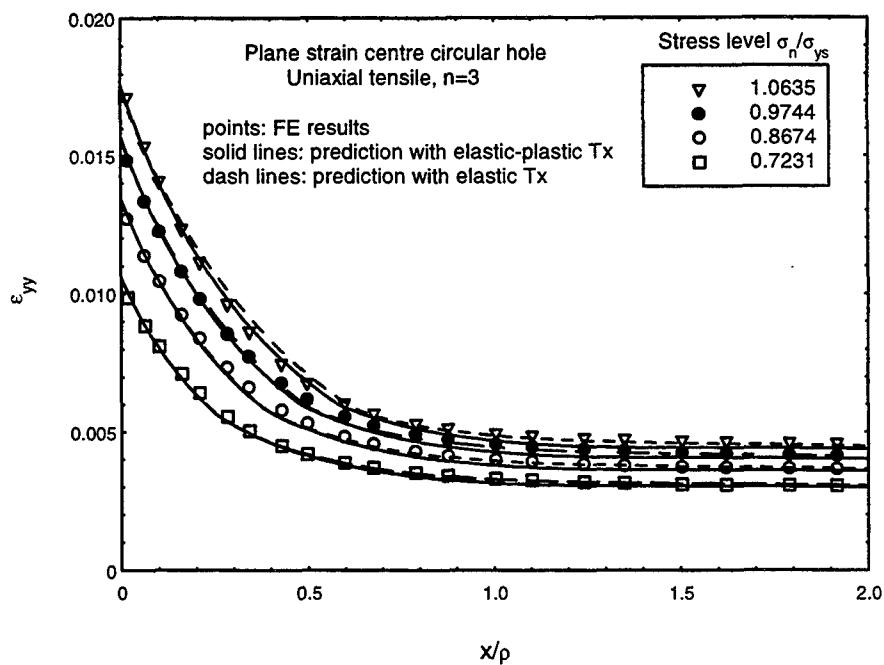


Figure 13: Prediction of strain ahead of the notch-tip in CASE 1.1

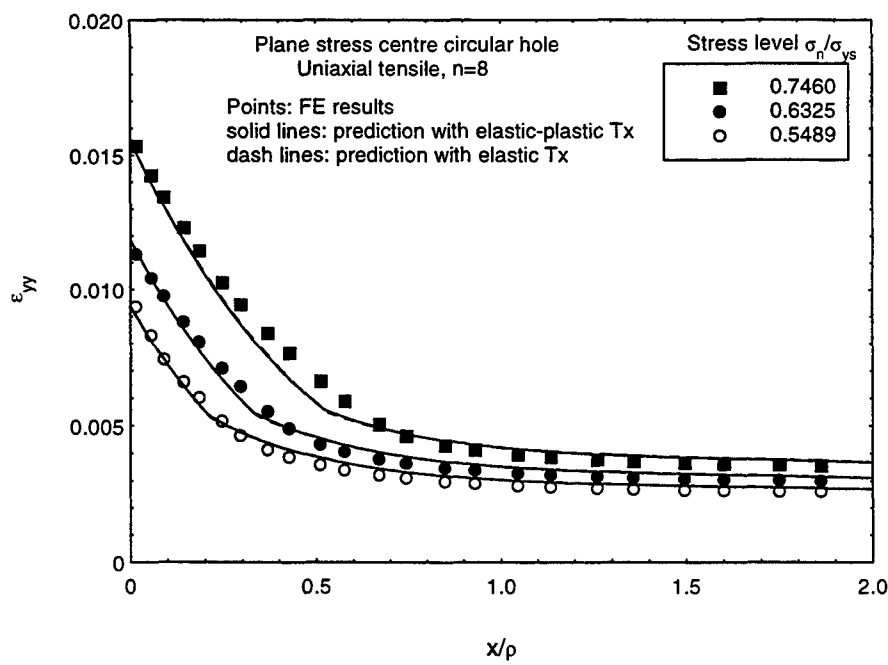
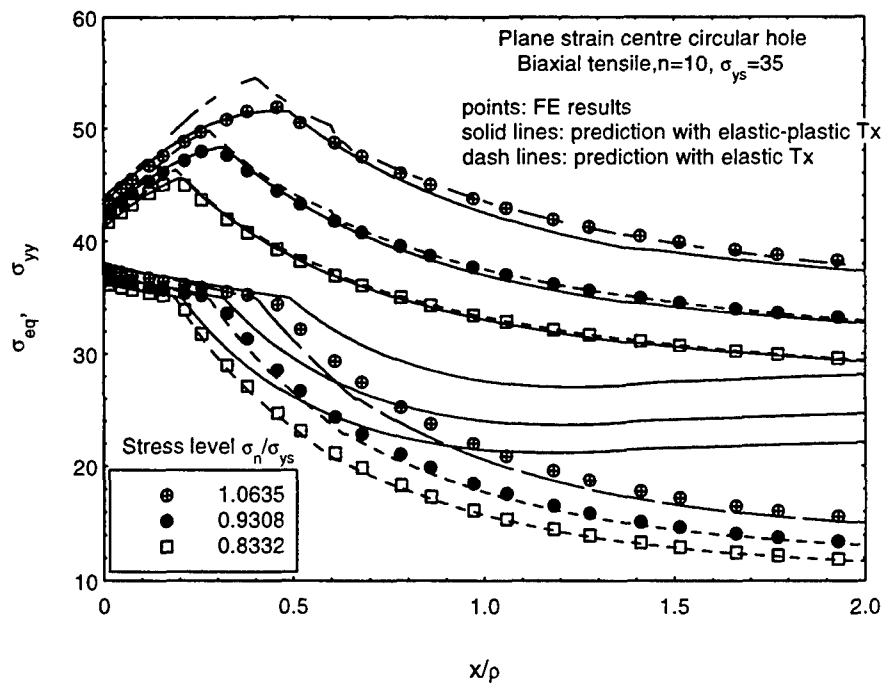
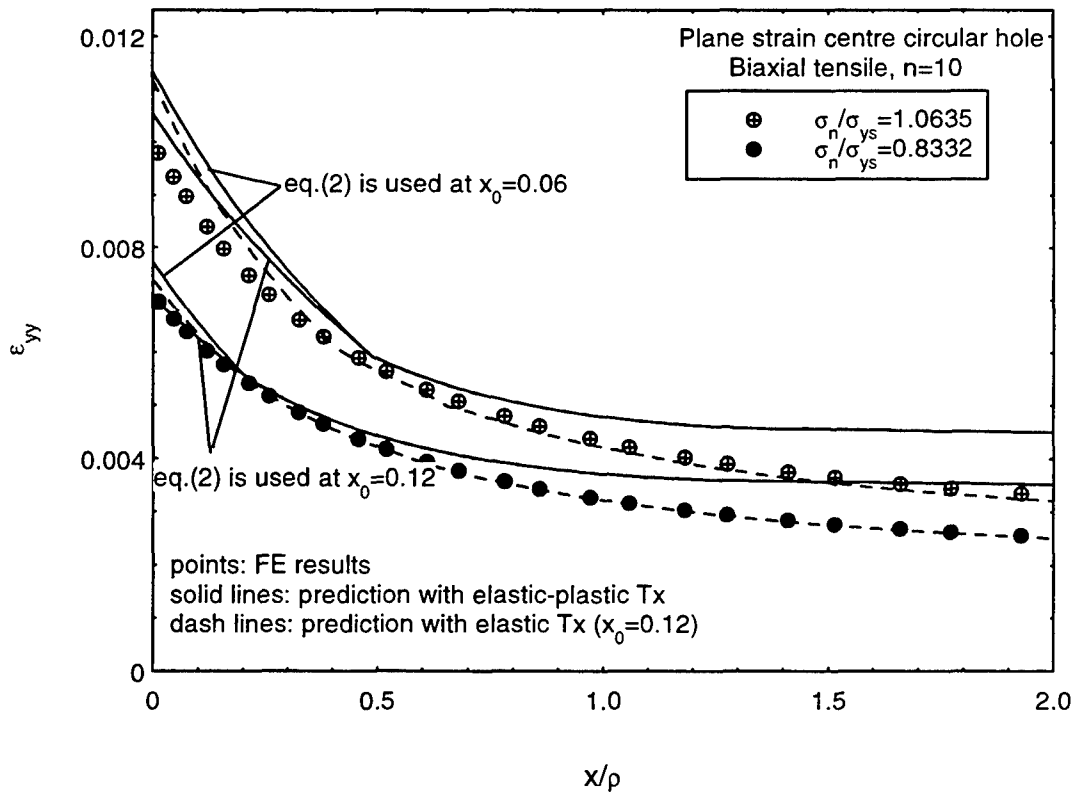


Figure 14: Prediction of strain ahead of the notch-tip in CASE 1.2

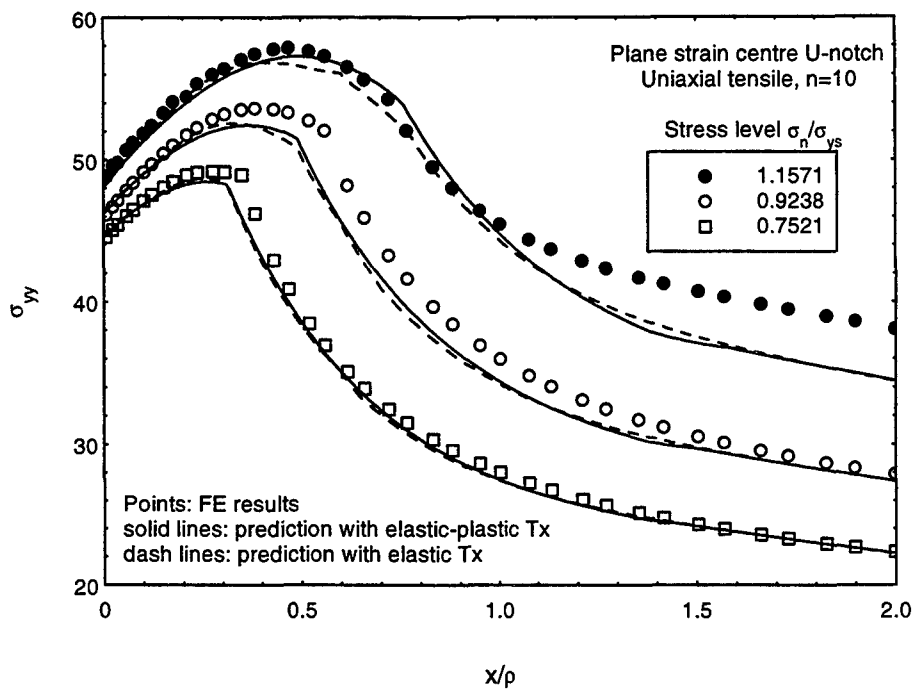


(a) prediction of stresses σ_{eq} and σ_{yy}

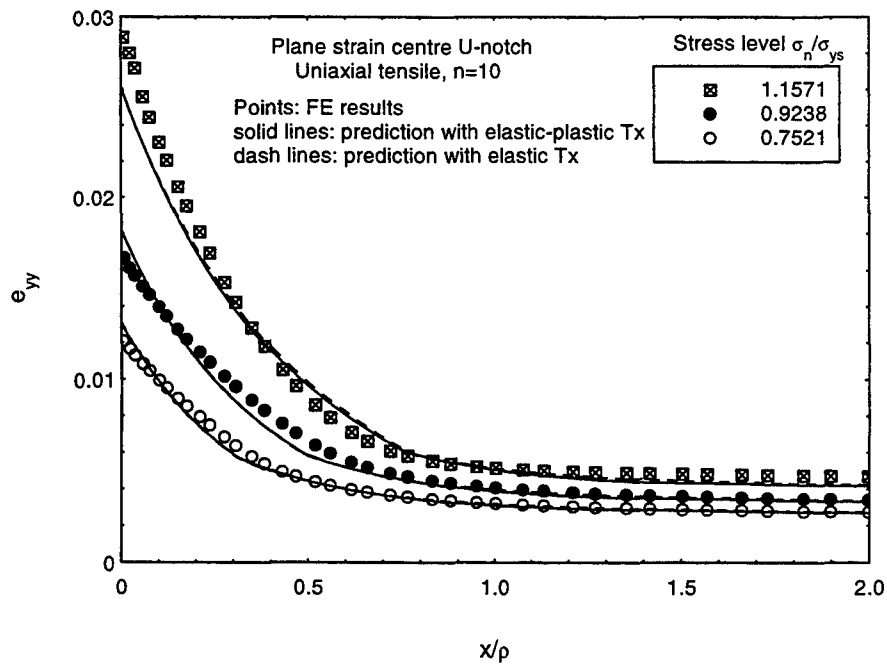


(b) prediction of strain ϵ_{eq}

Figure 15: Prediction of stresses (a) and strain (b) ahead of the notch-tip in CASE 1.3



(a)



(b)

Figure 16: Prediction of (a) stress and (b) strain ahead of the notch-tip in CASE 4

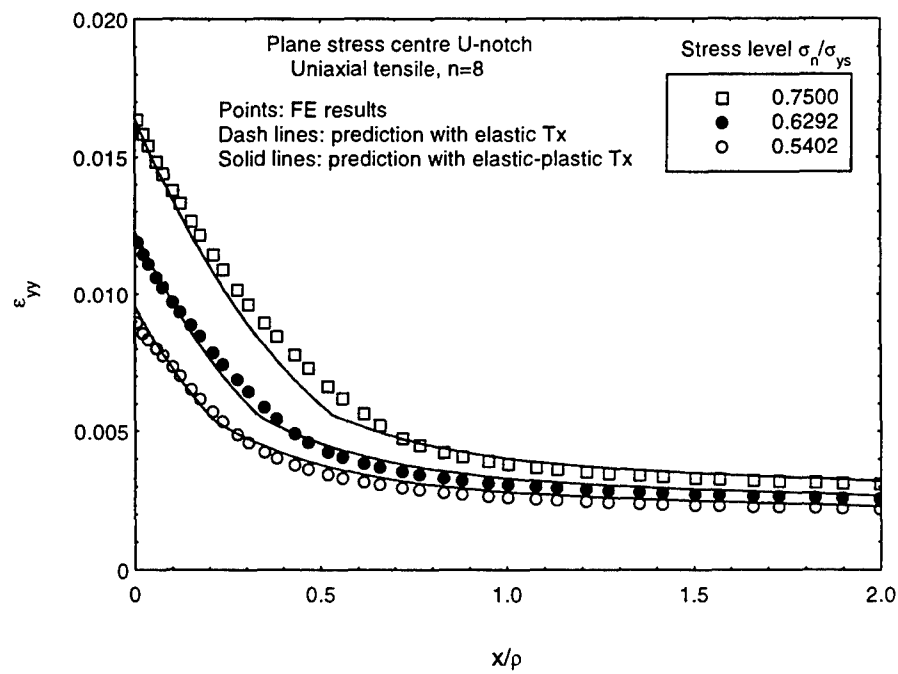


Figure 17: Prediction of strain ahead of the notch-tip in CASE 4.2

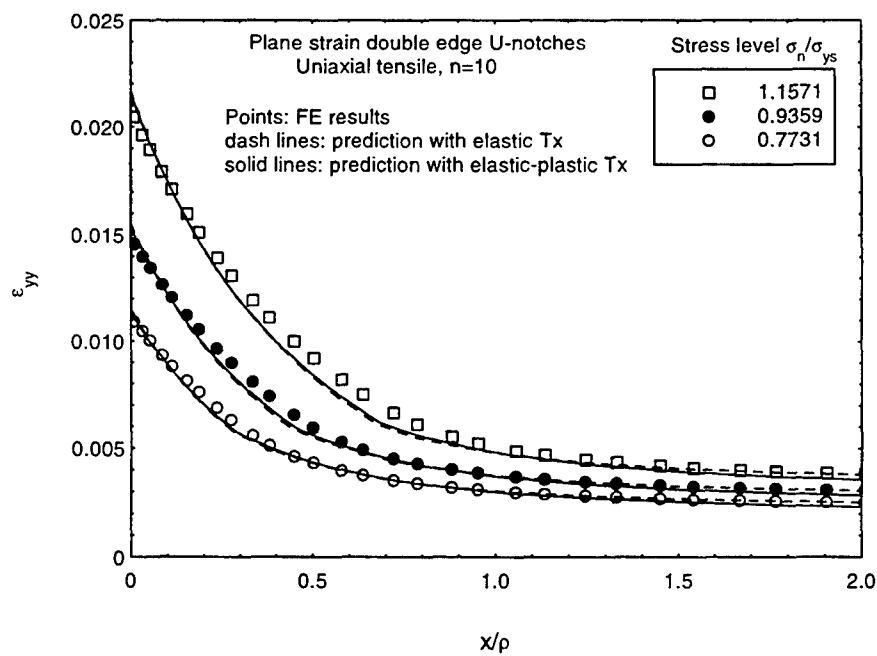


Figure 18: Prediction of strain ahead of the notch-tip in CASE 6

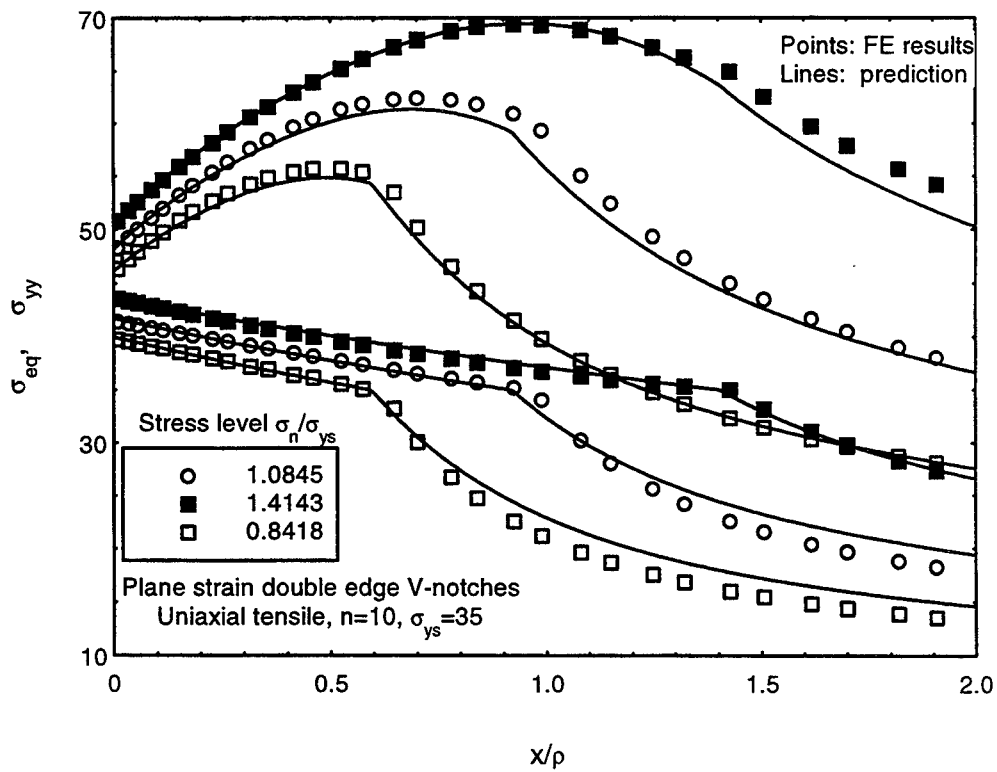
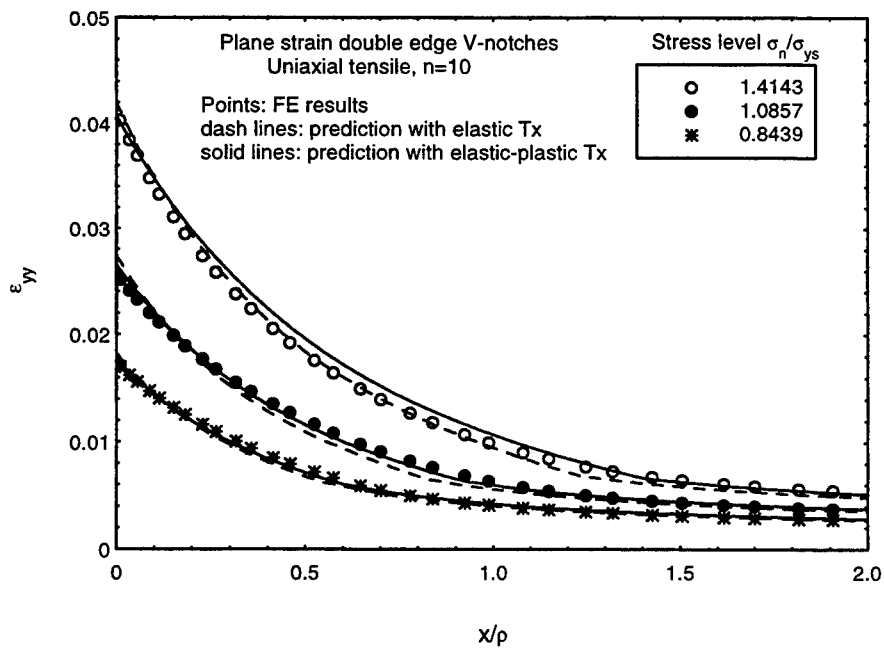
(a) prediction of stress σ_{yy} (b) prediction of strain ϵ_{yy}

Figure 19: Prediction of stress (a) and strain (b) ahead of the notch-tip in CASE 7

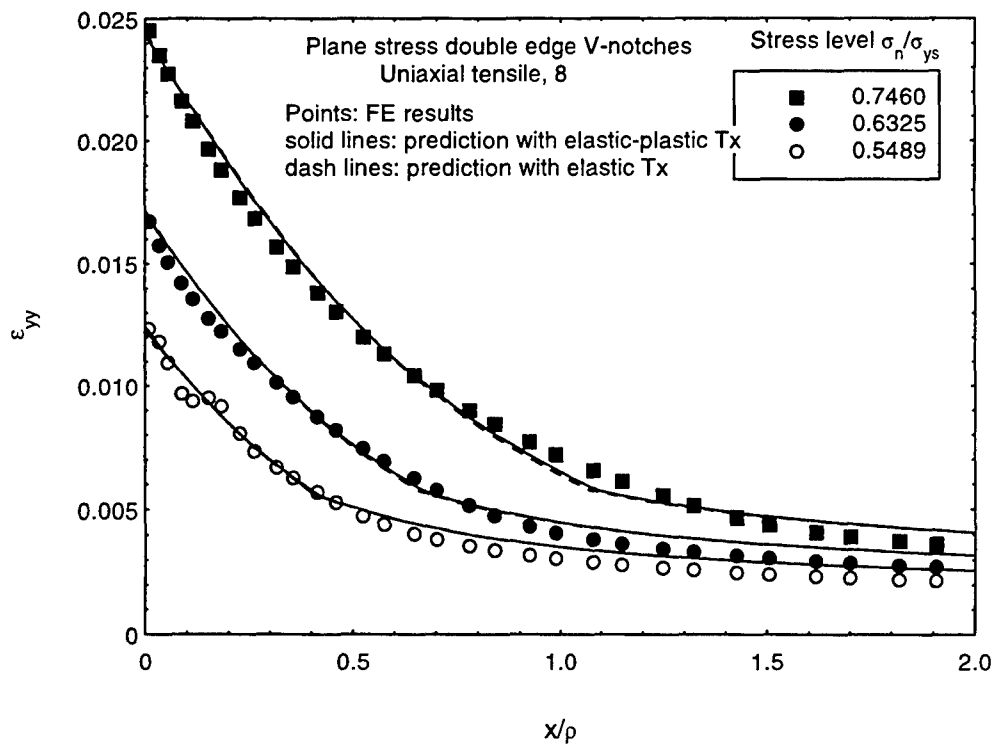
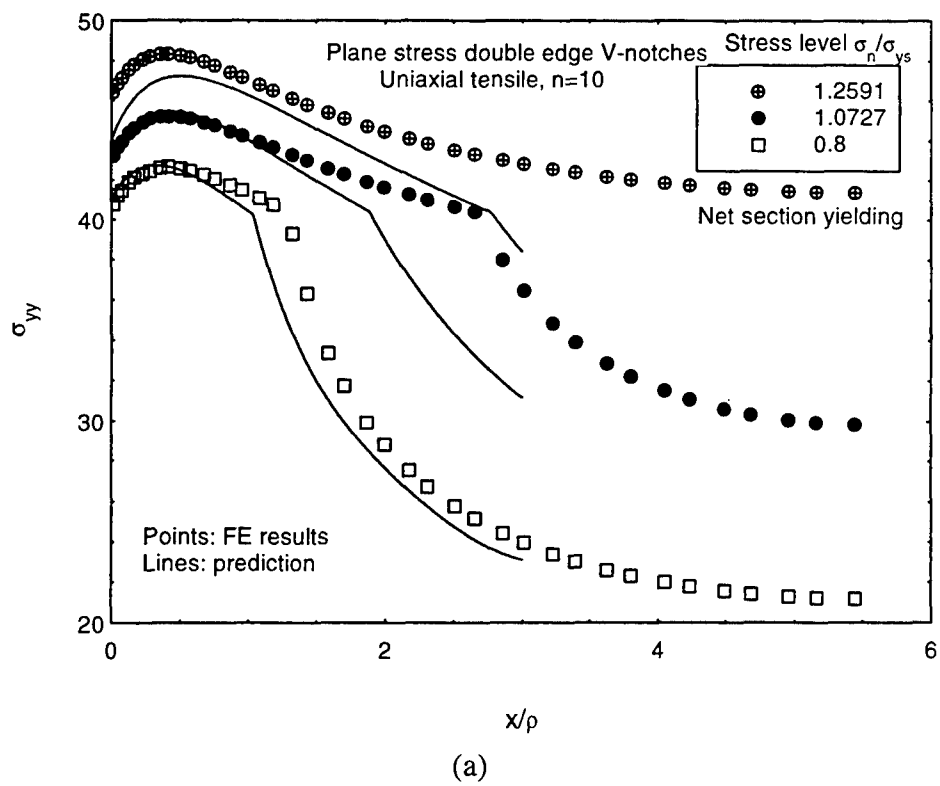
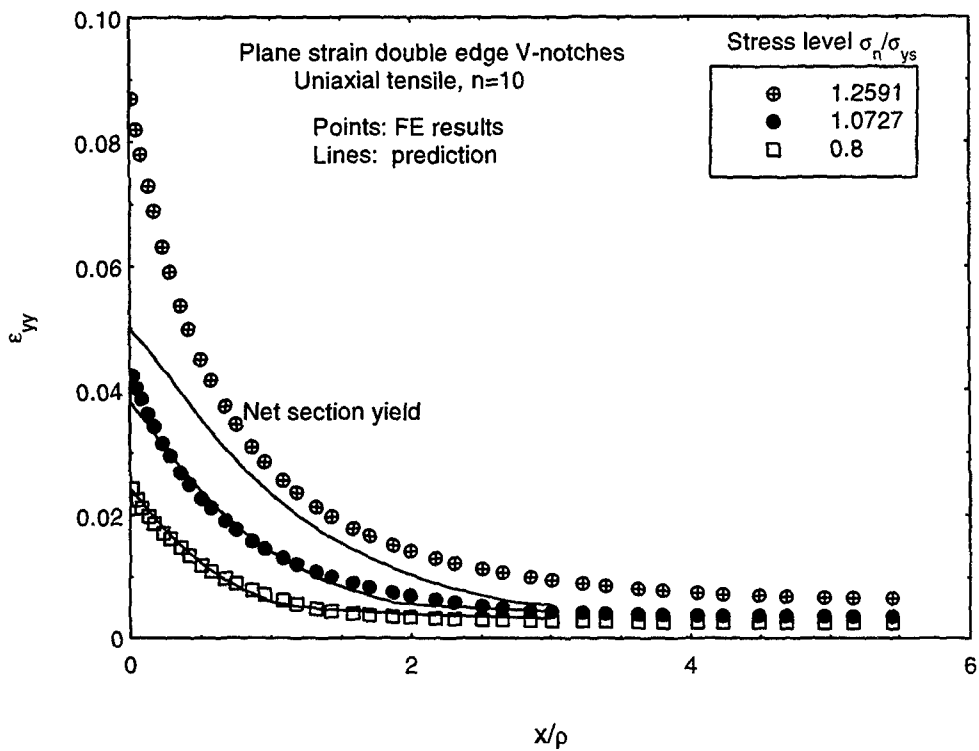


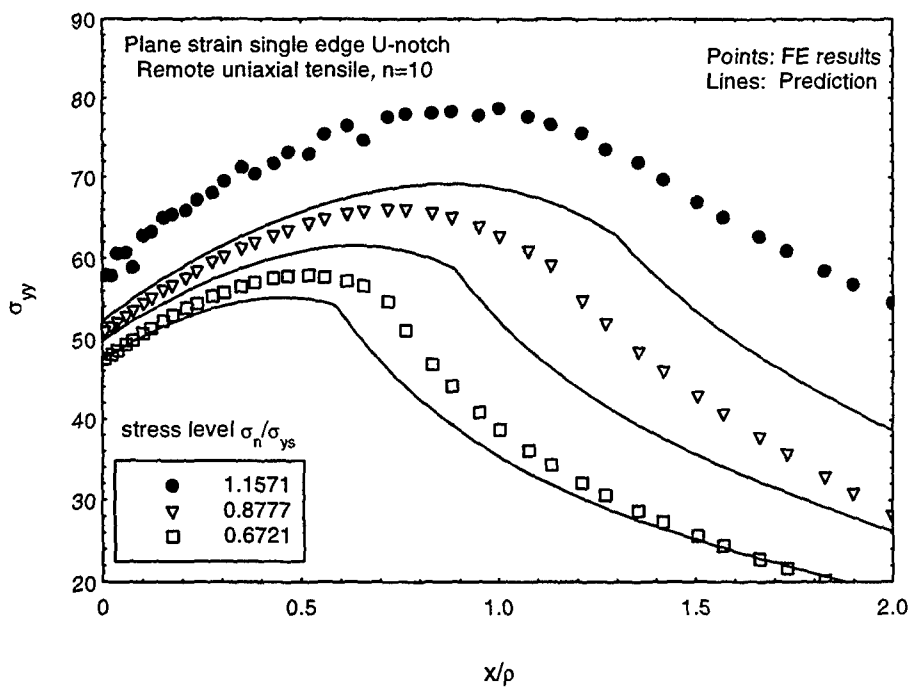
Figure 20: Prediction of strain ahead of the notch-tip in CASE 7.2





(b)

Figure 21: Prediction of stress (a) and strain (b) ahead of the notch-tip in CASE 82 at higher stress level



(a)

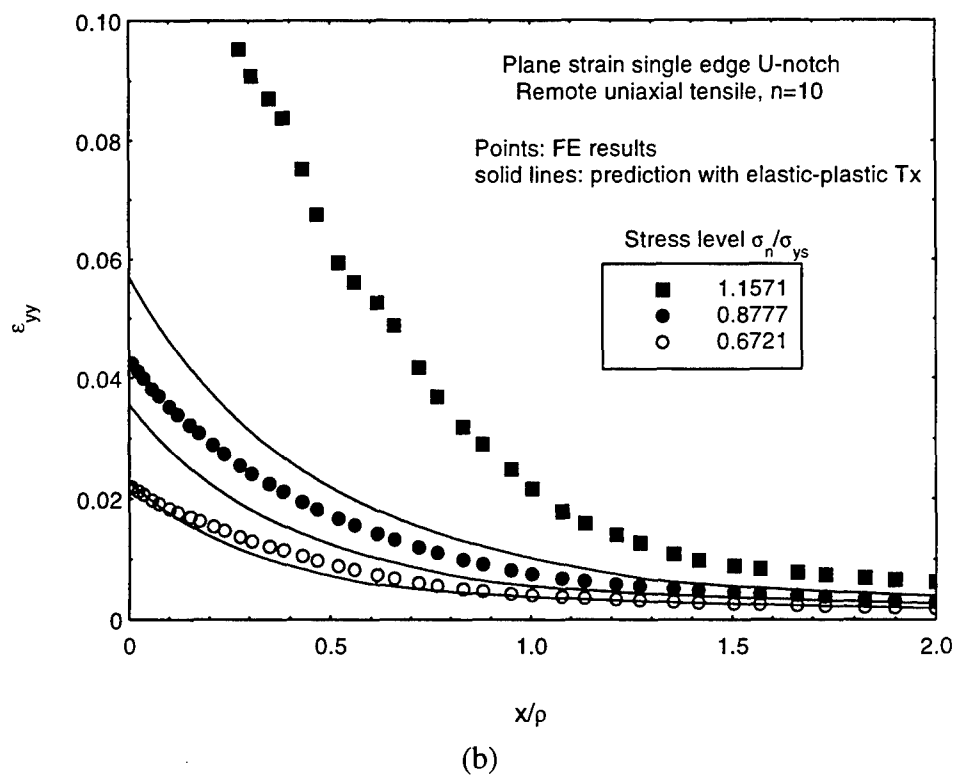


Figure 22: Prediction of stress (a) and strain (b) ahead of the notch-tip in CASE 5 at higher stress level

5. REFERENCES

1. Neuber, H. (1961) Theory of stress concentration for shear-strained prismatic bodies with arbitrary nonlinear stress-strain law, *J. Appl. Mech.*, Vol.23, 544-550.
2. Glinka, G. and Molski, K. (1981) A method of elastic-plastic stress and strain calculation at a notch root, *Mater. Sci. Engng*, Vol.50, 93-100.
3. Topper, T. H., Wetzell, R.M. and Morrow, J. (1969) Neuber's rule applied to fatigue of notched specimens, *J. Materials*, Vol.4, 200-209.
4. Gemma, A.E. (1985) An approximate elastoplastic analysis of the effect of plane strain at the surface of a notch, *Engng Fracture Mech.*, Vol.21, 495-501.
5. Hoffman, M. and Seeger, T. (1985) A generalised method for estimating multiaxial elastic-plastic notch stresses and strains-Part 1 and Part 2, *ASME J. Engng Mater. Tech.*, Vol.107, 250-260.
6. Glinka, G. (1985) Calculation of inelastic notch tip strain-stress histories under cyclic loading, *Engng Fracture Mech.*, Vol.22, 839-854.
7. Moftahar, A., Buczynski, A. and Glinka, G. (1995) Calculation of elastoplastic strains and stresses in notches under multiaxial loading, *Int. J. Fracture*, Vol.70, 357-373.
8. Singh, M.N.K., Glinka, G. and Dubey, R.N. (1996) Elastic-plastic stress-strain calculation in notched bodies subjected to non-proportional loading, *Int. J. Fracture*, Vol.76, 39-60.
9. Ball, D.L. (1990) Proposed integration of notch-strain and fatigue crack-growth analyses, *J. Aircraft*, Vol.27, 358-367.
10. Pilkey, W (1997) *Peterson's Stress Concentration Factors*, 2nd Edition, John Wiley, New York, USA.
11. Creager, M. and Paris, P.C. (1967) Elastic field equations for blunt cracks with reference to stress corrosion cracking, *Int. J. Fract. Mech.*, Vol.3, 247-252.
12. Glinka, G. and Newport, A. (1987) Universal features of elastic notch-tip stress fields, *Int. J. Fatigue*, Vol.9, 143-150.
13. Shin, C.S., Man, K.C. and Wang, C.M. (1994) A practical method to estimate the stress concentration of notches, *Int. J. Fatigue*, Vol.16, 242-256.
14. Lazzarin, P. and Tovo, R. (1996) A unified approach to the evaluation of linear elastic stress fields in the neighbourhood of cracks and notches, *Int. J. Fract.*, Vol.78, 3-19.
15. Timoshenko, S. and Goodier, J.N. (1970) *Theory of Elasticity*, McGraw Hill, New York, USA.
16. Hill, R. (1949) The plastic yielding of notched bars under tension, *Q.J. Mechanics and Applied Mathematics*, Vol.2, p.40-50.
17. Irwin, G. R. (1958) Fracture, *Handuch der Physik VI*, pp.551-590, Flugge Ed., Springer.
18. Wang, C. H. and Rose, L. R. F. (1998) Transient and Steady-state deformation at notch root under cyclic loading, *Mechanics of Materials* (accepted for publication).

DSTO-RR-0137

THIS PAGE BREAK PUT IN TO ALLOW FOR ODD AND EVEN HEADERS AND
FOOTERS ONLY.

DISTRIBUTION LIST

Elastoplastic Analysis of Notch-Tip Fields in Strain Hardening Materials

Wanlin Guo, C. H. Wang and L. R. F. Rose

AUSTRALIA

DEFENCE ORGANISATION

S&T Program

Chief Defence Scientist	}	shared copy
FAS Science Policy		
AS Science Corporate Management		
Director General Science Policy Development		
Counsellor Defence Science, London (Doc Data Sheet)		
Counsellor Defence Science, Washington (Doc Data Sheet)		
Scientific Adviser to MRDC Thailand (Doc Data Sheet)		
Director General Scientific Advisers and Trials/Scientific Adviser Policy and Command (shared copy)		
Navy Scientific Adviser (Doc Data Sheet and distribution list only)		
Scientific Adviser - Army (Doc Data Sheet and distribution list only)		
Air Force Scientific Adviser		
Director Trials		

Aeronautical and Maritime Research Laboratory

Director

Chief Airframes and Engines Division (CAED)

Authors:

C. H. Wang (5 copies)

L. F. R. Rose

W. Guo

K. Watters

K. Walker

L. Molent

W. Hu

D. Graham

DSTO Library

Library Fishermens Bend

Library Maribyrnong

Library Salisbury (2 copies)

Australian Archives

Library, MOD, Pyrmont (Doc Data sheet only)

Capability Development Division

Director General Maritime Development (Doc Data Sheet only)

Director General Land Development (Doc Data Sheet only)

Director General C3I Development (Doc Data Sheet only)

Army

ABCA Office, G-1-34, Russell Offices, Canberra (4 copies)
SO (Science), DJFHQ(L), MILPO Enoggera, Queensland 4051 (Doc Data Sheet only)
NAPOC QWG Engineer NBCD c/- DENGERS-A, HQ Engineer Centre Liverpool
Military Area, NSW 2174 (Doc Data Sheet only) Engineering Development
Establishment Library

Air Force

OIC ASI-LSA, DTA, HQLC

Intelligence Program

DGSTA Defence Intelligence Organisation

Corporate Support Program (libraries)

OIC TRS, Defence Regional Library, Canberra
Officer in Charge, Document Exchange Centre (DEC) (Doc Data Sheet and distribution list only)
*US Defence Technical Information Center, 2 copies
*UK Defence Research Information Centre, 2 copies
*Canada Defence Scientific Information Service, 1 copy
*NZ Defence Information Centre, 1 copy
National Library of Australia, 1 copy

UNIVERSITIES AND COLLEGES

Australian Defence Force Academy
Library
Head of Aerospace and Mechanical Engineering
Deakin University, Serials Section (M list), Deakin University Library, Geelong, 3217
Senior Librarian, Hargrave Library, Monash University
Librarian, Flinders University
LaTrobe University Library
University of Melbourne, Engineering Library
Newcastle University, Library
University of Sydney, Engineering Library
NSW, Physical Science Library
Queensland University, Library
Tasmania University, Engineering Library
University of Western Australia, Library

OTHER ORGANISATIONS

NASA (Canberra)
AGPS

OUTSIDE AUSTRALIA

ABSTRACTING AND INFORMATION ORGANISATIONS

INSPEC: Acquisitions Section Institution of Electrical Engineers
Library, Chemical Abstracts Reference Service
Engineering Societies Library, US
Materials Information, Cambridge Scientific Abstracts, US
Documents Librarian, The Center for Research Libraries, US

INFORMATION EXCHANGE AGREEMENT PARTNERS

Acquisitions Unit, Science Reference and Information Service, UK
Library - Exchange Desk, National Institute of Standards and Technology, US

SPARES (5 copies)

Total number of copies: 62

DEFENCE SCIENCE AND TECHNOLOGY ORGANISATION DOCUMENT CONTROL DATA									
				1. PRIVACY MARKING/CAVEAT (OF DOCUMENT)					
2. TITLE Elastoplastic Analysis of Notch-Tip Fields in Strain Hardening Materials			3. SECURITY CLASSIFICATION (FOR UNCLASSIFIED REPORTS THAT ARE LIMITED RELEASE USE (L) NEXT TO DOCUMENT CLASSIFICATION) Document (U) Title (U) Abstract (U)						
4. AUTHOR(S) Wanlin Guo, C. H. Wang and L. R. F. Rose			5. CORPORATE AUTHOR Aeronautical and Maritime Research Laboratory PO Box 4331 Melbourne Vic 3001 Australia						
6a. DSTO NUMBER DSTO-RR-0137		6b. AR NUMBER AR-010-615		6c. TYPE OF REPORT Research Report		7. DOCUMENT DATE August 1998			
8. FILE NUMBER M1/9/497		9. TASK NUMBER 98/192		10. TASK SPONSOR DST		11. NO. OF PAGES 35		12. NO. OF REFERENCES 18	
13. DOWNGRADING/DELIMITING INSTRUCTIONS none					14. RELEASE AUTHORITY Chief, Airframes and Engines Division				
15. SECONDARY RELEASE STATEMENT OF THIS DOCUMENT <i>Approved for public release</i> OVERSEAS ENQUIRIES OUTSIDE STATED LIMITATIONS SHOULD BE REFERRED THROUGH DOCUMENT EXCHANGE CENTRE, DIS NETWORK OFFICE, DEPT OF DEFENCE, CAMPBELL PARK OFFICES, CANBERRA ACT 2600									
16. DELIBERATE ANNOUNCEMENT No Limitations									
17. CASUAL ANNOUNCEMENT Yes									
18. DEFTTEST DESCRIPTORS Inelastic stresses, Plasticity theory, Fatigue, Fracture, Damage tolerance									
19. ABSTRACT The elastic-plastic fields near a notch tip in strain hardening materials are investigated and modelled for a wide range of notch configuration, geometry, and load levels. Two engineering methods that are commonly employed for determining the elastic-plastic response at a notch tip are first assessed, and the results indicate that Neuber's rule and its various extensions tend to overestimate the plastic strain at the notch-tip, and under-estimate the plastic strain away from the notch-tip. By contrast, the ESED method tends to underestimate the plastic strain at the notch-tip and its accuracy deteriorates as the load level increases. It is found that both methods are unable to provide satisfactory predictions of the stress-strain distribution ahead of a notch tip. To this end, an engineering approach is developed to characterise the stress-strain distribution in the notch-tip plastic zone, taking into account of the in-plane and through-thickness constraints near the notch root. Predictions are compared with finite element results, showing a good correlation for all the cases investigated.									